

1 **Indoxyl Sulfate, a Uremic Toxin, Induces Trained Immunity of Monocytes** 2 **through the AhR-Dependent Arachidonic Acid Pathway**

3
4 Hee Young Kim^{1,2,*}, Dong Hyun Kim³, Su Jeong Lee³, Yeon Jun Kang³, Gwanghun Kim⁴,
5 Hyun Mu Shin^{4,5}, Hajeong Lee⁶, Tae-Hyun Yoo⁷, and Won-Woo Lee^{1,2,3,8,*}

6
7 ¹ Department of Microbiology and Immunology, Seoul National University College of
8 Medicine, Seoul 03080, Republic of Korea.

9 ² Institute of Infectious Diseases, Seoul National University College of Medicine, Seoul
10 03080, Republic of Korea.

11 ³ Laboratory of Autoimmunity and Inflammation (LAI), Department of Biomedical Sciences,
12 and BK21Plus Biomedical Science Project, Seoul National University College of Medicine,
13 Seoul 03080, Republic of Korea.

14 ⁴ Department of Biomedical Sciences, College of Medicine and BK21Plus Biomedical
15 Science Project, Seoul National University College of Medicine, Seoul 03080, Republic of
16 Korea.

17 ⁵ Wide River Institute of Immunology, Seoul National University, Hongcheon 25159,
18 Republic of Korea.

19 ⁶ Division of Nephrology, Department of Internal Medicine, Seoul National University
20 Hospital, Seoul 03080, Republic of Korea.

21 ⁷ Division of Nephrology, Department of Internal Medicine, Yonsei University College of
22 Medicine, Seoul 03722 Republic of Korea.

23 ⁸ Ischemic/Hypoxic Disease Institute, Seoul National University College of Medicine; Seoul
24 National University Hospital Biomedical Research Institute, Seoul 03080, Republic of Korea.

25
26
27 * contributed equally
28
29

30 **Correspondence**

31
32 **Won-Woo Lee D.V.M., Ph.D.**

33 Professor,

34 Department of Microbiology and Immunology

35 Department of Biomedical Sciences

36 Seoul National University College of Medicine

37 103 Daehak-ro, Jongno-gu, Seoul 03080, South Korea.

38 Tel) +82-2-740-8303, Fax) +82-2-743-0881

39 E-mail) wonwoolee@snu.ac.kr

40
41 **Hee Young Kim Ph.D.**

42 Research Professor,

43 Department of Microbiology and Immunology

44 Seoul National University College of Medicine

45 103 Daehak-ro, Jongno-gu, Seoul 03080, South Korea.

46 Tel) +82-2-740-8545

47 E-mail) hyk0801@hotmail.com

48 **ABSTRACT**

49 Trained immunity is the long-term functional reprogramming of innate immune cells
50 following exposure to various insults that results in altered responses towards a secondary
51 challenge. Indoxyl sulfate (IS) is a potent uremic stimulus associated with inflammation in
52 chronic kidney disease (CKD). However, the impact of IS on trained immunity remains
53 unknown. Here, we find that IS induces trained immunity in monocytes *via* epigenetic and
54 metabolic reprogramming, resulting in augmented cytokine production upon LPS-
55 stimulation. Further, the aryl hydrocarbon receptor contributes to IS-trained immunity by
56 enhancing expression of arachidonic acid metabolism-related genes ALOX5 and ALOX5AP.
57 Monocytes from end-stage renal disease (ESRD) patients have increased ALOX5 expression
58 and healthy monocytes trained with uremic sera from ESRD patients exhibit increased TNF- α
59 and IL-6 production. Moreover, IS-trained mice have augmented TNF- α production
60 following LPS-stimulation. These results provide insight into the role of IS in trained
61 immunity, which is critical during inflammatory responses in CKD patients.

62 **Key Words:** Indoxyl Sulfate, Chronic Kidney Disease, Trained Immunity, Aryl Hydrocarbon
63 Receptor, Epigenetic and Metabolic Reprogramming

64 INTRODUCTION

65 Over the last decade, a large body of evidence has demonstrated that innate cells can
66 build up immunological memory resulting in enhanced responsiveness to subsequent
67 stimulation, a phenomenon termed trained immunity¹. Compared with classical epitope-
68 specific adaptive immunological memory based on an antigen-receptor, trained immunity of
69 monocytes and macrophages is the long-term functional reprogramming elicited by an initial
70 primary insult, mainly pathogen-associated molecular patterns (PAMPs), which leads to an
71 altered response towards a subsequent, unrelated secondary insult after the return to a
72 homeostatic state^{2,3}. It has been well demonstrated that exposure of monocytes or
73 macrophages to *Candida albicans*, fungal cell wall component β -glucan, or BCG (Bacille
74 Calmette-Guérin) vaccine enhances their subsequent responses to unrelated pathogens or
75 pathogen components such as lipopolysaccharide (LPS)^{4,5}. The induction of trained
76 immunity is associated with the interaction of epigenetic modifications and metabolic
77 rewiring, which can last for prolonged periods of time^{2,3,5,6,7,8}. Mechanistically, certain
78 metabolites derived from the upregulation of different metabolic pathways triggered by
79 primary insult can influence enzymes involved in remodeling the epigenetic landscape of
80 cells. This leads to specific changes in epigenetic histone markers, such as histone 3 lysine 4
81 trimethylation (H3K4me3) or histone 3 lysine 27 acetylation (H3K27ac), which regulate
82 genes resulting in a more rapid and stronger response upon a subsequent, unrelated secondary
83 insult^{2,3,4,7}. In addition, it has been recently reported that long non-coding RNAs induce
84 epigenetic reprogramming *via* the histone methyltransferase, MLL1. Subsequently,
85 transcription factors such as Runx1 regulate the induction of proinflammatory cytokines
86 following the secondary insult^{9,10,11}.

87 Many studies have provided evidence that trained immunity likely evolved as a
88 beneficial process for non-specific protection from future secondary infections³. However, it
89 has also been suggested that augmented immune responses resulting from trained immunity is
90 potentially relevant to deleterious outcomes in immune-mediated and chronic inflammatory
91 diseases such as autoimmune diseases, allergy, and atherosclerosis^{8, 10, 12, 13, 14, 15}. Thus,
92 although most studies have focused on the ability of exogenous microbial insults to induce
93 trained immunity, it is also conceivable that sterile inflammatory insults can evoke trained
94 immunity. In support of this idea, oxLDL, lipoprotein a (Lpa), uric acid, hyperglycemia, and
95 the Western diet have all been recently identified as endogenous sterile insults that induce
96 trained immunity in human monocytes *via* epigenetic reprogramming^{8, 10, 12, 13, 16}. Thus, it is
97 tempting to speculate that many endogenous insults that cause chronic inflammatory
98 conditions may be involved in the induction of trained immunity in human monocytes and
99 macrophages.

100 Chronic kidney disease (CKD) is recognized as a major non-communicable disease
101 with increasing worldwide prevalence^{17, 18}. Loss of renal function in CKD patients causes the
102 accumulation of over 100 uremic toxins, which are closely associated with cardiovascular
103 risk and mortality due to their ability to generate oxidative stress and a proinflammatory
104 cytokine milieu¹⁹. Reflecting this, cardiovascular disease (CVD) is a leading cause of death
105 among patients with end-stage renal disease (ESRD)²⁰. Indoxyl sulfate (IS) is a major uremic
106 toxin derived from dietary tryptophan *via* fermentation of gut microbiota²¹. Since it is poorly
107 cleared by hemodialysis, IS is one of the uremic toxins present at higher than normal
108 concentrations in the serum of CKD patients^{22, 23} and is associated with the progression of
109 CKD and the development of CKD-related complications such as CVD²⁴. We and others have

110 shown that IS promotes the production of proinflammatory cytokines such as TNF- α and IL-
111 1 β by monocytes and macrophages through aryl hydrocarbon receptor (AhR) signaling and
112 organic anion transporting polypeptides 2B1 (OATP2B1)-Dll4-Notch Signaling^{21, 25, 26},
113 suggesting a role of IS as an endogenous inflammatory insult in monocytes and macrophages.
114 Moreover, pretreatment with IS greatly increases TNF- α production by human macrophages
115 in response to a low dose of LPS²⁵. Despite the function of IS as an endogenous
116 inflammatory insult in monocytes and macrophages, little is known with regard to whether IS
117 induces trained immunity. Thus, we investigated whether exposure to IS triggers trained
118 immunity in an *in vitro* human monocyte model and an *in vivo* mouse model, as well as the
119 mechanisms involved in IS-induced trained immunity. Our data show that IS triggers trained
120 immunity in human monocytes/macrophages *via* AhR-dependent alteration of the arachidonic
121 acid (AA) pathway, epigenetic modifications, and metabolic rewiring. Thus, this suggests IS
122 plays a critical role in the initiation of inflammatory immune responses in patients with CKD.

123 **RESULTS**

124 ***Indoxyl sulfate (IS) induces trained immunity in human monocytes***

125 To explore whether exposure to IS is involved in the induction of trained immunity in
126 human monocytes, an *in vitro* model of trained immunity was applied as previously reported
127 by the Netea group⁴. Freshly isolated human monocytes were preincubated for 24 hrs with or
128 without IS and, after a subsequent 5-day culture in human serum, restimulated with
129 lipopolysaccharide (LPS) or Pam3cys for final 24 hrs (Fig. 1A). Preincubation of monocytes
130 with IS led to enhanced production of TNF- α , a major monocyte/macrophage-derived
131 inflammatory cytokine, upon LPS stimulation. Since 10 ng/ml of LPS significantly increased
132 both TNF- α and IL-6 secretion in IS-pretreated macrophages (Fig. 1B), we used this
133 concentration of LPS in subsequent experiments. The preincubation effect of IS on cytokine
134 production was observed at a concentration as low as 250 μ M, which is the average IS
135 concentration in patients with ESRD in our cohort (Fig. 1C)²⁵. Unlike IS, preincubation with
136 other protein-bound uremic toxins (PBUTs), such as *p*-cresyl sulfate (PCS), Hippuric acid
137 (HA), Indole 3-acetic acid (IAA) and kynurenic acid (KA), did not cause increased secretion
138 of TNF- α or IL-6 in response to LPS stimulation (Fig. S1A). In addition, there was no
139 obvious effect on cell viability following pre-incubation of macrophages with 1,000 μ M of IS
140 after a subsequent 5-day culture in human serum or after LPS stimulation (Fig. S1B). We also
141 found that the enhanced cytokine production of IS-pretreated macrophages was not
142 attributable to potassium derived from IS potassium salt (Fig. S1C). Moreover, the increased
143 TNF- α and IL-6 production in IS-pretreated macrophages was not limited to LPS stimulation,
144 as similar phenomena were observed following stimulation with Pam3cys, a TLR1/2 agonist
145 (Fig. 1D). β -glucan-pretreated macrophages exhibit a prototypic feature of trained immunity,

146 characterized by enhanced production of inflammatory cytokines upon restimulation with
147 heterologous stimuli, LPS or Pam3cys^{6,27}. As seen in Figure S1D, the level of TNF- α
148 secreted by IS-pretreated macrophages was comparable with that secreted by β -glucan-
149 trained macrophages, although β -glucan had a more potent effect on IL-6 production than did
150 IS, suggesting that IS plays a role in the induction of trained immunity of human monocytes.
151 In addition to TNF- α and IL-6, mRNA expression of IL-1 β and MCP-1 (CCL2) was
152 significantly increased in IS-pretreated macrophages, whereas the anti-inflammatory cytokine
153 IL-10 was greatly reduced in the same cells (Fig. 1E). These results suggest that IS induces
154 trained immunity in human monocytes, characterized by the increased expression of
155 proinflammatory cytokines TNF- α and IL-6 and reduced expression of anti-inflammatory IL-
156 10 in response to secondary TLR stimulation.

157 ***Epigenetic modifications control IS-induced trained immunity.***

158 The induction of trained immunity relies on two key, closely intertwined
159 mechanisms, epigenetic modification and metabolic rewiring of innate immune cells^{2,28,29}.
160 We first sought to determine whether increased expression of TNF- α and IL-6 is a result of
161 epigenetic changes. To this end, chromatin modification of histone 3 trimethylation of lysine
162 4 (H3K4me3) at the promoter sites of *TNFA* and *IL6* was analyzed. Chromatin
163 immunoprecipitation (ChIP)-qPCR data illustrate that IS-trained macrophages exhibit
164 enhanced H3K4me3 of *TNFA* and *IL6* promoters by day 6 after IS treatment (Fig. 2A and B).
165 This reflects what was previously demonstrated in trained innate immune cells^{4,22,30}.
166 Moreover, IS-mediated enrichment of H3K4me3 was maintained even after secondary
167 stimulation with LPS compared with non-trained cells (Fig. S2A-B). When IS-trained
168 macrophages were pretreated with 5'-methylthioadenosine (MTA), a non-selective

169 methyltransferase inhibitor, their production of TNF- α and IL-6 upon LPS stimulation was
170 reversed to baseline (Fig. 2C), implying that IS-induced trained immunity is associated with
171 epigenetic modification. To further elucidate epigenetic modifications in IS-induced trained
172 immunity, we performed a whole-genome assessment of the histone marker H3K4me3 by
173 ChIP-sequencing (ChIP-Seq) in IS-trained cells on day 6. Among 7,136 peaks, 59
174 differentially upregulated peaks and 316 downregulated peaks were detected in IS-trained
175 cells (Fig. 2D and Table S1). To identify the biological processes affected in IS-mediated
176 trained immunity, 59 upregulated peaks in IS-trained macrophages were analyzed through
177 Gene Ontology (GO) analysis with Go biological process and the Reactome Gene Set.
178 Activation of the innate immune response and positive regulation of the defense response
179 were identified as major processes *via* Go biological process analysis. Further, genes
180 involved in regulation of ornithine decarboxylase (ODC) and metabolism of polyamine were
181 recognized as major gene sets *via* Reactome Gene Set analysis (Fig. 2E). A genome browser
182 snapshot showing H3K4me3 binding illustrates that H3K4me3 is elevated at the promoters of
183 important target genes associated with activation of the innate immune response, such as
184 IFI16 (interferon-gamma inducible protein 16), XRCC5 (X-ray repair cross-complementing
185 5), and PQBP1 (polyglutamine binding protein 1) and genes linked to the regulation of
186 ornithine decarboxylase (ODC), such as PSMA1 (proteasome 20S subunit alpha 1), PSMA3
187 (proteasome 20S subunit alpha 3), and OAZ3 (Ornithine Decarboxylase Antizyme 3, a
188 protein that negatively regulates ODC activity) (Fig. 2F)³¹. Our results show that epigenetic
189 modification of innate immune response-related genes contributes to the induction of IS-
190 trained immunity in human monocytes.

191 ***IS-induced trained immunity is regulated by metabolic rewiring.***

192 Metabolic rewiring is one of the most crucial processes regulating trained immunity
193 of monocytes and macrophages³². Assessment of the metabolic profile of IS-trained
194 macrophages on day 6 (prior to restimulation with LPS) showed that training with IS led to
195 an enhanced extracellular acidification rate (ECAR) as a measure of lactate production and
196 resultantly, glycolysis and glycolysis capacity were increased (Fig. 3A and B). Moreover,
197 basal and maximal respiration and ATP production gauged by the oxygen consumption rate
198 (OCR) were also increased compared to that of non-trained cells (Fig. 3C and D). Enhanced
199 glycolysis and glycolytic capacity in IS-trained cells remained higher even after re-
200 stimulation with LPS (Fig. S2A-B), implying that the IS-training effect on metabolic rewiring
201 is sustained regardless of the secondary stimulation. To further examine whether the
202 metabolic rewiring by IS-trained cells is linked to the regulation of trained immunity, 2-
203 deoxy-d-glucose (2-DG), a general inhibitor of glycolysis, was added to monocytes before
204 training with IS. 2-DG completely inhibited the augmented production of TNF- α and IL-6 in
205 IS-trained macrophages in response to re-stimulation with LPS (Fig. 3E). Our findings were
206 corroborated by the finding that on day 6 IS-trained macrophages showed an enhanced
207 enrichment of H3K4m3 on promoter sites of *HK2* and *PFKP*, major glycolysis-related genes
208 (Fig. S2C). These data demonstrate that IS-trained immunity is linked to metabolic rewiring
209 characterized by both enhanced glycolysis and augmented oxidative respiration.

210 ***AhR, a potent endogenous receptor for IS, contributes to the induction of IS-trained***
211 ***immunity.***

212 Our previous study demonstrated that IS-induced TNF- α production in macrophages
213 is regulated through a complicated mechanism involving the interaction of NF- κ B and
214 SOCS2 with AhR²⁵. To explore the molecular mechanism underlying the regulation of IS-

215 trained immunity, we investigated the role of AhR, a potent endogenous receptor for IS.
216 Ligand-bound activated AhR is known to be immediately translocated into the nucleus and
217 rapidly degraded^{25, 33, 34, 35}. Immunoblot data in Figure 4A shows that IS-mediated
218 degradation of AhR was not fully recovered even on day 6 (prior to restimulation with LPS)
219 and was completely inhibited by treatment with GNF351, an AhR antagonist, on day 6.
220 Inhibition of AhR by GNF351 during IS training suppressed the increase in production of
221 TNF- α and IL-6 following LPS restimulation on day 6 in IS-trained cells (Fig. 4B and C),
222 implying that IS-mediated AhR activation may be involved in trained immunity. In addition
223 to TNF- α and IL-6, enhancement of IL-1 β and MCP-1 mRNA expression in IS-trained cells
224 was also completely inhibited, whereas decreased IL-10 expression was completely reversed
225 by GNF351 (Fig. 4D). To confirm the regulatory role of AhR in trained immunity, we tested
226 whether 6-Formylindolo[3,2-b]carbazole (FICZ), a tryptophan-derived agonist of AhR, also
227 induced trained immunity in human monocytes. FICZ-pretreated monocytes exhibited
228 augmented expression of TNF- α and IL-6 in response to secondary stimulation with LPS
229 compared to non-trained cells (Fig. S4A). Thus, this suggests an important role of ligand-
230 bound activated AhR in the trained immunity of human monocytes. We next examined
231 whether inhibition of AhR with GNF351 influences epigenetic modification and metabolic
232 rewiring. Our CHIP-qPCR assay showed that enrichment of H3K4m3 on *TNFA* and *IL6*
233 promoters in IS-trained macrophages was inhibited by GNF351 (Fig. 4E). Of note,
234 assessment of the metabolic profile by measuring ECAR and OCR illustrates that GNF351
235 has no effect on metabolic rewiring, including enhanced glycolysis and mitochondrial
236 respiration, in IS-trained cells on day 6 as depicted in Figure 3 (Fig. S4B-C). This finding
237 was corroborated by the immunoblotting data, which showed GNF351 had no inhibitory
238 effect on IS-mediated enhancement of S6K activity, which is critical for inducing the aerobic

239 glycolysis in human monocytes/macrophages (Fig. S4D). Our findings suggest that IS-
240 activated AhR is involved in regulating epigenetic modifications of IS-trained macrophages.

241 ***AhR-dependent induction of the arachidonic acid pathway is involved in IS-induced***
242 ***trained immunity***

243 To explore which molecular mechanism is involved in the induction of IS-trained
244 immunity, we performed RNA-sequencing (RNA-Seq) on day 6 (prior to restimulation with
245 LPS) in IS-trained human macrophages. A total of 218 differentially expressed genes (DEGs),
246 consisting of 71 upregulated and 147 downregulated genes, were identified in IS-trained
247 macrophages compared to non-trained cells (Fig. 5A and B; $FC \geq \pm 2$, $p < 0.05$). Gene
248 ontology (GO) analysis of these expression data using the Reactome Gene Set is displayed in
249 Figure 5C. IS-trained macrophages had upregulated pathways including those involved in
250 neutrophil degranulation, integrin cell surface interactions, extracellular matrix organization
251 and arachidonic acid metabolism, whereas pathways associated with kinesins, cell cycle, and
252 the $G\alpha(i)$ signaling pathway were downregulated (Fig. 5C). Considering the key role of the
253 arachidonic acid (AA) pathway in many inflammatory disorders, we decided to focus on this
254 pathway in the induction of trained immunity by IS. Our findings were supported by Gene
255 Set Enrichment Analysis (GSEA) using Molecular Signatures Database (MsigDB), in which
256 genes related to AA metabolism were enriched in IS-trained macrophages compared to non-
257 trained cells and more importantly, upregulated expression of these genes was inhibited by
258 treatment with GNF351 as illustrated by heatmap analysis of major genes related to AA
259 metabolism (Fig. 5D and E and Fig. S5E). Among AA metabolism pathways, the leukotriene
260 metabolic process, but not the cyclooxygenase (COX) pathway, was primarily involved in the
261 induction of IS-mediated trained immunity (Fig. S5A). Confirmatory RT-qPCR analysis on

262 major AA metabolism-related genes was conducted using IS-trained macrophages obtained
263 from independent, HCs (Fig. 5F). The mRNA expression of arachidonate 5-lipoxygenase
264 (ALOX5: also known as 5-LOX or 5-LO) and arachidonate 5-lipoxygenase activating protein
265 (ALOX5AP: also known as FLAP), the enzymes catalyzing AA into leukotrienes (a group of
266 pro-inflammatory lipid mediators)^{36, 37, 38}, was higher in IS-trained macrophages than non-
267 trained cells. In addition, the mRNA expression of LTB4R1 (also known as BLT1), a high-
268 affinity receptor for leukotriene B4 (LTB4), was also upregulated. The augmented expression
269 of these AA metabolism-related genes was repressed by GNF351 pretreatment as shown by
270 changes in expression of CYP1B1, a typical AhR target gene. Thus, this suggests that the IS-
271 activated AhR pathway is involved in enhanced AA-metabolism in IS-induced trained
272 immunity. Immunoblot analysis confirmed that the expression of ALOX5 and ALOX5AP is
273 upregulated in IS-trained immunity and is inhibited by GNF351 at the protein level (Fig. 5G).

274 We previously reported alterations in the transcriptome signature of monocytes
275 treated with IS for 24 hr and *ex vivo* monocytes of ESRD patients³⁹. Comparison of the fold
276 changes of RNA-Seq data in the present study and microarray data reported previously
277 (GSE155325 and GSE155326) revealed that the expression of ALOX5 and LTB4R1 is
278 enhanced in IS-trained macrophages and *ex vivo* monocytes of ESRD patients, but not in IS-
279 treated monocytes, for 24 hr (Fig. S5B). Differential expression of ALOX5, ALOX5AP, and
280 LTB4R1 shown by transcriptome analysis (Fig. S5B) were confirmed by RT-qPCR (Fig. 5F
281 and Fig. S5C). To further investigate the roles of the AA metabolism pathway in IS-trained
282 immunity, Zileuton, an ALOX5 inhibitor, and U75302, a BLT1 receptor inhibitor were used
283 during the induction of trained immunity by IS (Fig. S5D). We found that IS-induced TNF- α
284 and IL-6 production were largely suppressed by both zileuton and U75302 (Fig. 5H-I).

285 Therefore, these findings suggest that AA metabolism plays an important role in the induction
286 of IS-trained immunity.

287 Histone-modifying enzymes such as lysine demethylase (KDM) and lysine
288 methyltransferase (KMT) are linked to the induction of trained immunity by remodeling the
289 epigenetic status of cells^{3,4}. However, RNA-Seq data of IS-trained macrophages showed no
290 obvious change in the expression profile of major histone-modifying enzymes (Fig. S6A). In
291 agreement with this, mRNA expression of major histone modifying enzymes including
292 KDM5A, KDM5B, KDM5C, Setdb2, SETD7, and SETD3 were not changed in IS-trained
293 macrophages on day 6 (Fig. S5B)^{4, 40, 41, 42}. Treatment with MTA, a non-selective
294 methyltransferase inhibitor, partially inhibited expression of ALOX5 and ALOX5AP mRNA
295 (Fig. 5J), suggesting limited epigenetic regulation of the AA pathway (Fig. 5J).

296 ***Ex vivo* and *in vivo* validation of IS-induced trained immunity**

297 Circulating monocytes have been identified as a major immune cell subset that
298 responds to IS in the serum of ESRD patients^{21, 25}. To examine whether uremic serum induces
299 trained immunity of monocytes/macrophages, pooled sera from ESRD patients ($184 \pm 44 \mu\text{M}$
300 of average IS level) or from HCs were used to treat monocytes isolated from HCs for 24 hr at
301 30% (v/v), followed by training for 5 days. Treatment with pooled uremic serum of ESRD
302 patients increased the production of TNF- α and IL-6 upon restimulation with LPS compared
303 to monocytes treated with the pooled sera of HCs (Fig. 6A-B). In addition, expression of IL-
304 1 β and MCP-1 mRNA was also augmented by treatment with the pooled uremic sera of
305 ESRD patients (Fig. S7A). We next tested whether treatment with uremic serum leads to
306 increased expression of AA pathway-related genes within 6 days (prior to restimulation with

307 LPS) as found in IS-trained macrophages. The expression of ALOX5, ALOX5AP, and
308 LTB4R1 mRNA was augmented by treatment with pooled uremic sera of ESRD patients
309 compared with HCs (Fig. 6C), and this augmented expression was maintained after re-
310 stimulation with LPS (Fig. S7B). Since peripheral monocytes in ESRD patients are
311 chronically exposed to uremic toxins like IS, we examined whether *ex vivo* monocytes
312 purified from ESRD patients before hemodialysis exhibit features of IS-trained macrophages.
313 The expression of ALOX5, but not ALOX5AP, in *ex vivo* monocytes of ESRD patients was
314 significantly increased at the protein level compared with that of age-matched HCs (Fig. 6D-
315 E). Moreover, monocyte-derived macrophages (MDMs) from ESRD patients also had higher
316 expression of ALOX5 compared to MDMs of HCs (Fig. 6F-G), suggesting that IS in serum
317 of ESRD patients contributes to the induction of trained immunity of
318 monocytes/macrophages.

319 To examine the biological relevance of IS-trained immunity, we adopted a murine
320 model in which IS was intraperitoneally injected daily for 5 days, followed by training for
321 another 5 days and then restimulation with 5 mg/kg LPS for 75 min (Fig. 6H). The level of
322 TNF- α in serum was increased in IS-trained mice compared to that of control mice (Fig. 6I).
323 To further examine the effect of IS-training on innate responses, splenic myeloid cells were
324 isolated after 5 days of training (prior to injection with LPS) followed by *in vitro* stimulation
325 with 10 ng/ml LPS for 24 h. The amount of TNF- α in the supernatant was augmented
326 following culture with LPS-stimulated mouse splenic myeloid cells derived from IS-trained
327 mice compared the control condition (Fig. 6J). Finally, we found that the expression of
328 ALOX5 was upregulated in *ex vivo* splenic myeloid cells of IS-treated mice compared to
329 control mice (Fig. 6K), similar to what was observed in monocytes and macrophages from

330 ESRD patients (Fig. 6E-G). Together, these data provide evidence for the role of IS and the
331 induction of the AA pathway in the establishment of trained immunity of monocytes and
332 macrophages both *ex vivo* and *in vivo*.

333 **DISCUSSION**

334 The capability to develop adaptive features in innate immune cells, a *de facto*
335 memory response, is an evolutionarily conserved trait that enhances the fitness of plants,
336 invertebrates, and vertebrates against pathogenic microbes⁴³. Conceptually, this innate
337 memory most likely evolved as a beneficial immune process to improve host defense against
338 reinfections^{3, 44}. Recent studies have shown that BCG-induced trained immunity has
339 protective effects against unrelated secondary infections, both viral and bacterial, including
340 COVID-19^{45, 46}. BCG vaccination has also been shown to induce antitumor effects with
341 elimination of cancers including bladder cancer and melanoma through efficient activation of
342 the immune system⁴⁷. On the other hand, a maladaptive or successive effect of trained
343 immunity can be potentially detrimental in immune-mediated and chronic inflammatory
344 diseases¹⁵. Several studies have reported that endogenous sterile inflammatory insults
345 including ox-LDL, hyperglycemia and uric acid, trigger trained immunity and contribute to
346 chronic inflammation in cardiovascular diseases and gout^{8, 10, 12, 16}. Here, our study provides
347 evidence that IS, a major uremic toxin, provokes trained immunity in human
348 monocytes/macrophage through epigenetic modification, metabolic rewiring, and AhR-
349 dependent induction of the AA pathway, suggesting its important role in inflammatory
350 immune responses in patients with CKD (Fig. 7).

351 Chronic kidney disease (CKD) is pervasive, affecting 8-16% of the population
352 worldwide¹⁷. CKD is associated with increased risk factors of cardiovascular disease (CVD)
353 including traditional risk factors, such as hypertension, age and dyslipidemia, as well as non-
354 traditional risk factors, such as oxidative stress and inflammation^{23, 48}. Further, recent cohort
355 studies have shown that CKD is an independent risk factor for CVD⁴⁸. Since CVD is the

356 major cause of death in patients with ESRD, therapeutic manipulation of risk factors
357 associated with CVD is important to reduce the associated mortality and morbidity^{49, 50}.
358 Uremia accompanying renal failure causes immune dysfunction, which is closely linked to
359 the pathogenesis of CKD-related CVD⁵¹. Among over 100 uremic toxins identified, IS is a
360 prototypical protein-bound uremic toxin most likely to be participating in progressive
361 pathophysiology of CVD including endothelial dysfunction, vascular calcification, and
362 increased atherosclerosis^{21, 26, 49, 52}. Immunologically, IS activates monocytes and
363 macrophages and enhances the production of their proinflammatory cytokines, TNF- α and
364 IL-1 β , *via* AhR signaling^{21, 25}. IS-induced activation of AhR/Nuclear factor erythroid-2-
365 related factor2 (Nrf2) axis promotes monocyte differentiation into profibrotic macrophages⁵³
366 and the progression of atherosclerosis and calcification is accelerated by IS-mediated
367 activation of proinflammatory macrophages through Dll4-Notch signaling²⁶. Mounting
368 evidence suggests that a prolonged hyperactivation of trained immunity is intimately related
369 to the pathogenesis of atherosclerosis, the major contributor to cardiovascular diseases.
370 Oxidized low-density lipoprotein (oxLDL), hyperglycemia, and the Western diet, all known
371 to be associate with the progression of atherosclerosis, have been reported to induce trained
372 immunity through epigenetic reprogramming^{8, 10, 12}. These findings suggest that IS plays a
373 role as a typical endogenous inflammatory insult in activating monocytes and macrophages
374 and modulating their responses. Given that IS is difficult to clear by hemodialysis, this toxin
375 has a chronic effect on the immune system of patients. Nonetheless, little is known about the
376 effects of IS on trained immunity.

377 Our previous studies have revealed that pretreatment with IS markedly augmented
378 TNF- α production by human macrophages in response to a low dose of LPS and IS-bound

379 AhR activation is likely linked to this phenomenon²⁵. This prompted us to examine the
380 possible role of IS as a trigger of trained immunity of human monocytes. As observed using a
381 common *in vitro* model of trained immunity established by Netea and other groups (Fig. 1A),
382 CD14⁺ monocytes, which are exposed for 24 h to the first insult with IS and rested for 5 days
383 without IS, produced an augmented level of TNF- α and IL-6 and decreased level of IL-10 in
384 response to an unrelated second insult with LPS or Pam3cys, which is a feature typical of
385 trained immunity of monocytes (Fig. 1B-E). Mechanistic studies have demonstrated that the
386 induction of trained immunity is coordinated through the interplay of epigenetic
387 modifications and metabolic rewiring, which is broadly characterized as prolonged changes
388 in transcription programs and cell physiology that do not involve permanent genetic changes,
389 such as the mutations and recombination events crucial for adaptive immunity². In the present
390 study, ChIP-Seq and real-time metabolic analysis show that the induction of IS-trained
391 immunity in human monocytes is attributable to epigenetic modification and metabolic
392 rewiring (Fig. 2 and 3). Consistent with previous findings^{5, 12}, trimethylation of histones at
393 H3K4 on *TNFA* and *IL6* promoters was increased in IS-trained macrophages and maintained
394 even after secondary stimulation with LPS (Fig. 2B and Fig. S2B). Furthermore, the
395 production of TNF- α and IL-6 upon LPS stimulation was completely inhibited by
396 pretreatment with 5'-methylthioadenosine (MTA), a methyltransferase inhibitor (Fig. 2C),
397 demonstrating that IS-induced trained immunity is associated with epigenetic modification.
398 Moreover, H3K4me3-ChIP-Seq data showed that IS-induced trained immunity accompanied
399 by epigenetic reprogramming and H3K4me3 was enriched in genes related to activation of
400 the innate immune responses as illustrated by gene ontology (GO) analysis (Fig. 2D-E).

401 Here, we identified AhR as a critical mediator of IS-trained immunity in human
402 monocytes (Fig. 4). AhR is a ligand-activated nuclear transcription factor (TF), which is
403 activated by several exogenous compounds, such as benzo[a]pyrene environmental pollutants
404 and 2,3,7,8-tetrachloro-dibenzo-*p*-dioxin (TCDD), as well as by multiple endogenous ligands
405 including tryptophan and indole metabolites⁵⁴. AhR plays a multifaceted role in modulating
406 cellular mechanisms such as inflammation, cell growth, and antioxidant responses⁵⁵.
407 Mounting evidence has shown that AhR is involved in the regulation of cellular metabolism
408 in many types of cells by acting as a TF to control the expression of metabolism-related
409 genes, by interacting with intracellular signaling pathways related to metabolism, or by
410 disturbing mitochondrial function^{56, 57}. AhR is expressed by various immune cells, and its
411 signaling exerts integrative effects on the cellular environment and metabolism of the
412 immune responses⁵⁸. However, little is known about the role of AhR in the induction of
413 trained immunity.

414 AhR has been identified as a potent endogenous receptor for IS in human
415 monocytes/macrophages and is responsible for IS-mediated proinflammatory responses^{21, 25,}
416 ³³. In the present study, we show that IS-trained immune responses, characterized by the
417 expression of proinflammatory cytokines and chemokines, were inhibited by GNF351, an
418 AhR antagonist (Fig. 4B-D), accompanied by repression of enriched H3K4me3 on *TNFA* and
419 *IL6* promoters in IS-trained macrophages (Fig. 4E), indicating an AhR-dependent
420 mechanism. However, increased glycolysis and mitochondria respiration in IS-trained
421 macrophages were not suppressed by the blockade of AhR activation with GNF351,
422 suggesting the AhR activation is not directly involved in metabolic rewiring in IS-trained
423 immunity (Fig. S4B-C). It has been demonstrated that metabolic rewiring, especially

424 upregulation of aerobic glycolysis and the TCA cycle, is a major mechanism underlying the
425 induction of trained immunity, and metabolites such as mevalonate and fumarate generated
426 from this metabolic rewiring can in turn regulate epigenetic modification⁴³. Although
427 inducers of trained immunity, such as β -glucan, BCG, uric acid, and oxLDL, initiate
428 intracellular signaling and metabolic pathways, each *via* different receptors, the most
429 common pathway is the Akt/mTOR/HIF1 α -dependent induction of aerobic glycolysis^{3, 15, 43}.
430 Our data also revealed that training with IS led to enhanced glycolysis, which is critical for
431 the production of TNF- α and IL-6 upon LPS stimulation as confirmed by experiments with
432 2DG, a glycolysis inhibitor (Fig. 3E). Recent studies have shown that IS activates mTORC1
433 in a variety of cells such as epithelial cells, fibroblasts, and THP-1 cells mainly *via* the
434 Organic Anion Transporters (OAT)/NADPH oxidase/ROS pathway, but not the AhR
435 pathway⁵⁹. Our findings suggest that IS-trained macrophages acquire the characteristics of
436 trained immunity by AhR-dependent and -independent mechanisms and enhances
437 proinflammatory responses upon secondary stimulation. Thus, addressing the mechanism
438 underlying AhR-independent metabolic rewiring in IS-trained macrophages will require
439 further investigations.

440 A finding of particular interest in our study is that the induction of IS-induced trained
441 immunity is dependent on the AhR-ALOX5/ALOX5AP axis, as depicted by RNA-Seq
442 analysis and confirmatory *in vitro* analysis of mRNA and protein expression (Fig. 5 and Fig.
443 S5). ALOX5 and ALOX5AP are major rate-limiting enzymes associated with the arachidonic
444 acid (AA) pathway, involved in the production of leukotrienes, proinflammatory lipid
445 mediators derived from AA³⁷. Among leukotrienes, leukotriene B4 (LTB4), an extremely
446 potent inflammatory mediator, binds to G protein-coupled protein, LTB4R, and enhances

447 inflammatory responses by increased phagocytosis and activation of the signaling pathway
448 for the production of cytokines^{36, 38}. Mechanistically, the LTB₄-LTB₄R signaling pathway
449 induces the PI3K/Akt or NF- κ B pathways^{60, 61}. AhR-dependent LTB₄ production through
450 enhanced ALOX5 expression in hepatocytes reportedly induces hepatotoxicity *via* neutrophil
451 infiltration⁶². We found that AhR-dependent ALOX5 expression was induced at 6 days (prior
452 to restimulation with LPS), and not at day 1, after IS treatment of human monocytes (Fig. 5
453 and S5B-C). The increase in ALOX5 activity and LTB₄ expression has been reported in
454 patients with ESRD^{63, 64, 65} and ALOX5 mediates mitochondrial damage and apoptosis in
455 mononuclear cells of ESRD patients⁶³. Thus, antagonists of ALOX5/ALOX5AP have been
456 used for treatment in CKD⁶⁵. Consistent with these findings, peripheral monocytes derived
457 from ESRD patients in our cohort have increased expression of ALOX5 and this increase was
458 maintained after differentiation into macrophages with M-CSF (Fig. 6D-G). Considering that
459 pretreatment with the uremic serum of ESRD patients elicits a change in gene expression and
460 cytokine production as observed in IS-trained macrophages, it is likely that increased ALOX5
461 in monocytes and macrophages of ESRD patients is mediated by IS in uremic serum. Our
462 previous studies have shown that IS is an important uremic toxin in the serum of ESRD
463 patients that elicits proinflammatory responses of monocytes²¹. Furthermore, the AhR-
464 ALOX5-LTB₄R1 pathway is involved in IS-induced trained immunity of patients with
465 ESRD.

466 Murine models have been widely used to investigate the specific contribution of
467 inducers of trained immunity and the underlying mechanisms to a long-term functional
468 modification of innate cells *in vivo*^{7, 42, 66}. Mice trained with β -glucan enhance the production
469 of proinflammatory cytokines such as TNF- α , IL-6, and IL-1 β by monocytes and

470 macrophages in response to secondary microbial stimuli and subsequently obtain increased
471 protection against various microbial infections^{15, 43}. Our *in vivo* and *ex vivo* mouse
472 experiments for trained immunity demonstrate that IS-trained immunity has biological
473 relevance (Fig. 6I). Previous studies have shown that intraperitoneal injection of exogenous
474 IS into wild-type C57BL/6 mice leads to an increase of IS in the plasma until 3~6 hr post-
475 injection despite its rapid excretion by the kidney. In this period, the expression of pro-
476 inflammatory, pro-oxidant, and pro-apoptotic genes in peritoneal macrophages was
477 upregulated^{59, 67}. Moreover, intraperitoneal injection of IS daily for 3 days elevates IS in the
478 plasma of mice and activates the mTORC1 signaling pathway in the mouse kidney⁵⁹. This
479 suggests that the IS-injected mouse model is suitable for investigating the mechanisms
480 underlying IS-mediated immune responses. Our data show increased TNF- α and IL-6 in
481 serum after injection of LPS (Fig. 6I). Moreover, ALOX5 protein expression was increased in
482 splenic myeloid cells derived from IS-trained mice and *ex vivo* stimulation with LPS for 24 hr
483 induced TNF- α expression in these splenic myeloid cells (Fig. 6J-K). Thus, this suggests a
484 systemic induction of IS-trained immunity in the mouse model.

485 In conclusion, the current study provides new insight into the role of IS as an inducer
486 of trained immunity as well as the underlying mechanisms in human monocytes/macrophages
487 by investigating the effect of IS *in vivo* and *in vitro* using experimental models of trained
488 immunity. Here, we demonstrate that IS, a major uremic toxin, induces trained immunity
489 characterized by the increased proinflammatory TNF- α and IL-6 in human monocytes
490 following secondary stimulation through epigenetic modification and metabolic rewiring. IS-
491 mediated activation of AhR is involved in the induction of trained immunity through
492 enhanced expression of arachidonic acid (AA) metabolism-related genes such as ALOX5 and

493 ALOX5AP. Monocytes from patients with ESRD exhibit increased expression of ALOX5 and
494 their uremic serum causes HC-derived monocytes to increase the production of TNF- α and
495 IL-6 upon LPS restimulation, implying IS-mediates trained immunity in patients. Supporting
496 our *in vitro* findings, mice trained with IS and their splenic myeloid cells had increased
497 production of TNF- α after *in vivo* and *ex vivo* LPS stimulation. These results suggest that IS
498 plays an important role in the induction of trained immunity, which is critical in inflammatory
499 immune responses in patients with CKD and thus, it holds potential as a therapeutic target.

500 MATERIALS AND METHODS

501 Cell preparation and culture

502 Study protocols were reviewed and approved by the IRB (institutional review board)
503 of Seoul National University Hospital and Severance Hospital. Peripheral blood of ESRD
504 patients and healthy controls (HCs) was drawn after obtaining written, informed consent. The
505 methods were performed in accordance with the approved guidelines. Peripheral blood
506 mononuclear cells (PBMCs) were isolated from peripheral blood by density gradient
507 centrifugation (Bicoll-Separating Solution; BIOCHROM Inc, Cambridge, UK). Monocytes
508 were positively purified from PBMCs with anti-CD14 magnetic beads (Miltenyi Biotec Inc,
509 Auburn, CA). For *in vitro* trained immunity experiments, purified monocytes were treated
510 with IS for 24 h, followed by washing with pre-warmed PBS and incubation for another 5
511 days in RPMI medium supplemented with 10% human AB serum (HS, Sigma-Aldrich, St.
512 Louis, MO), 100 U/ml penicillin, and 100 µg/ml streptomycin (Gibco, Grand Island, NY). On
513 day 6, cells were re-stimulated with LPS or Pam3cys for 24 hr and the supernatants and their
514 lysates were collected and stored at -80°C until use. In some experiments, chemical inhibitors
515 were used for a 1 hr pre-treatment at the indicated concentrations prior to the treatment with
516 IS. To test the effect of uremic serum on the induction of trained immunity, CD14⁺
517 monocytes purified from HC donors were seeded into 48-well plates and incubated for 24 hr
518 at 30% (v/v) with the pooled uremic sera (US) from ESRD patients or the pooled normal sera
519 (NS) from HCs, followed by washing with pre-warmed PBS and incubation for another 5
520 days. On day 6, cells were re-stimulated with LPS for 24 hr. In some experiments, monocyte-
521 derived macrophages (MDMs) were differentiated from purified CD14⁺ monocytes from
522 ESRD patients or age-matched HCs in RPMI 1640 medium supplemented with 10% fetal

523 bovine serum (FBS, BioWest, Nuaille, France), 50 ng/ml recombinant human M-CSF
524 (PeproTech, Rocky Hill, NJ, USA), 100 U/ml penicillin, and 100 mg/ml streptomycin. On
525 day 6, MDMs were used for immunoblot analysis.

526 **Chemicals and antibodies**

527 Indoxyl sulfate (IS) potassium salt, GNF351, 5'-methylthioadenosine (MTA), 2-
528 deoxy d-glucose (2DG), and zileuton were purchased from Sigma-Aldrich (Burlington, MA,
529 USA). Lipopolysaccharides (LPS) from E. coli 0111: B4 were purchased from InvivoGen
530 (San Diego, CA, USA) for *in vitro* experiments and Sigma-Aldrich for *in vivo* experiments.
531 U-75302 was obtained from Cayman Chemical (Ann Arbor, Michigan, USA). Anti-AhR and
532 anti-5-loxygenase (5-LOX) antibodies (Ab) for immunoblot assay and anti-trimethyl H3K4
533 (H3K4me3) Ab for chromatin immunoprecipitation (ChIP) were purchased from Cell
534 Signaling Technology (Danvers, MA, USA). Anti-ALOX5AP (FLAP) antibody was obtained
535 from Abcam Inc. (Cambridge, UK).

536 **Enzyme-linked immunosorbent assay (ELISA)**

537 The amounts of TNF- α and IL-6 in culture supernatants of LPS or Pam3cys-re-
538 stimulated IS-trained macrophages were quantified using commercial human ELISA kits
539 (Thermo Fisher Scientific, Waltham, MA, USA). Optical density was measured using the
540 Infinite M200 (Tecan, Männedorf, Switzerland).

541 **Quantitative RT-PCR**

542 Total RNA was prepared using RNA purification kit (Macherey-Nagel GmbH & Co.
543 KG, Germany), followed by cDNA synthesis (Bio-line, London, UK), and then real-time

544 quantitative RT-PCR was performed with the CFX system (Bio-Rad, Hercules, CA) using the
545 SensiFAST SYBR® Lo-ROX (Bio-line, London, UK). Sequences of primers used in this
546 investigation are shown in Table S2. Normalization of gene expression levels against the
547 expression of ACTINB using the comparative CT method ($\Delta\Delta CT$) was used for quantification
548 of gene expression.

549 **ChIP-qPCR and ChIP-Seq**

550 Cells were washed with Dulbecco's PBS and crosslinked for 5 min with 1%
551 formaldehyde at room temperature (RT), followed by quenching with 100 mM glycine for 5
552 min. Cells were harvested with lysis buffer (50 mM HEPES, pH7.5, 140 mM NaCl, 1 mM
553 EDTA, 10% glycerol, 0.5% NP-40 and 0.25% Triton X-100) with protease inhibitors on ice
554 for 10 min and were then washed with washing buffer (10 mM Tris-HCl, pH7.0, 200 mM
555 NaCl, 1 mM EDTA, and 0.5 mM EGTA) for 10 min. The lysates were resuspended and
556 sonicated in sonication buffer (10 mM Tris-HCl, pH8.0, 100 mM NaCl, 1 mM EDTA, 0.5
557 mM EGTA, 0.1% sodium deoxycholate and 0.5% N-laurolsarcosine) using a Bioruptor®
558 (diagenode, Denville, NJ) with 30s on and 30s off on a high-power output for 25 cycles. After
559 sonication, samples were centrifuged at 12,000 rpm for 10 min at 4 °C and 1% sonicated cell
560 extracts were saved as input. Cell extracts were incubated with protein A agarose loaded with
561 the H3K4me3 Ab overnight at 4 °C, and then Ab-bound agarose beads were washed twice
562 with sonication buffer, once with sonication buffer with 500 mM NaCl, once with LiCl wash
563 buffer (10 mM Tris-HCl, pH8.0, 1 mM EDTA, 250 mM LiCl and 1% NP-40), and once with
564 TE with 50 mM NaCl. After washing, DNA was eluted in freshly prepared elution buffer (1%
565 SDS and 0.1 M NaHCO₃). Cross-links were reversed by overnight incubation at 65°C with
566 RNase A, followed by incubation with proteinase K for 1 hr at 60°C. DNA was purified with

567 NucleoSpin™ gDNA Clean-up Kit (Macherey-Nagel GmbH & Co. KG, Germany). For
568 ChIP-qPCR assays, immunoprecipitated DNA was analyzed by quantitative real-time PCR
569 and results were normalized against input DNA. The sequences of primers used for ChIP-
570 qPCR are shown in Table S3^{5,68}.

571 For ChIP-seq experiments, purified DNA were prepared for DNA libraries using
572 TruSeq DNA Sample Prep Kit according to Library Protocol TruSeq ChIP Sample
573 Preparation Guide 15023092 Rev. B. Next, illumina sequencing were performed using
574 NovaSeq 6000 S4 Reagent Kit according to sequencing protocol of NovaSeq 6000 System
575 User Guide Document # 1000000019358 v02. Sequenced reads were trimmed using
576 Trimmomatic software. Fragments were aligned to hg19 using Bowtie2 software. Aligned
577 fragments of H3K4me3-ChIP samples were concatenated into a single file to generate
578 consistent peak ranges between samples using the makeTagDirectory function of Homer
579 Suite. For each sample, regions of H3K4me3 enrichment compared to the input sample were
580 collected using callpeaks function in MACS3 software. H3K4me3-rich regions from the same
581 group of different donors were compared to peaks in linked samples using the findoverlap
582 function of the GenomicRange R-package, and 11,123 peaks were collected for further
583 analysis. For quantitative comparisons between IC-trained groups and controls, the number of
584 fragments of each peak in BEDPE was collected using the coverage function of the BEDtools
585 software. Then, the number of fragments in the peak was normalized to CPM and
586 significance was compared using edgeR R-package. Finally, we selected 7,136 peaks with at
587 least 15 CPM from the larger average group to exclude lowly H3K4me3 enriched peaks.

588 Enriched peaks were selected base on a *p*-value of 0.05 or less and log₂ fold change
589 of > 1.3. The selected enriched peaks were used for Go pathway analysis. Pathway analysis

590 was conducted using Metascape web-based platform⁶⁹ and significant pathways were
591 identified on the basis of Go biological process and Reactome gene sets. Significant pathways
592 were selected with $p < 0.05$ and enrichment score (ES) > 1.5 .

593 **RNA-sequencing (RNA-Seq) and analysis**

594 After RNA extraction, libraries for sequencing were prepared using the TruSeq
595 Stranded mRNA LT Sample Prep Kit and sequencing were performed using NovaSeq 6000
596 System User Guide Document # 1000000019358 (Illumina). To analyze RNA-Seq data,
597 trimmed reads were aligned to the human GRCh37 (NCBI_105.20190906). Gene expression
598 profiling was performed using StringTie and then read count and FPKM (Fragment per
599 Kilobase of transcript per Million mapped reads) were acquired. Differentially expressed
600 genes (DEGs) were selected based on p -value of 0.05 or less. Selected data were applied to
601 hierarchical cluster analysis to display basal and luminal differences and were further filtered
602 according to gene expression levels with a log₂ fold change of < -2 and > 2 . DEGs were
603 visualized using the R (ver. 4.1.1) and pheatmap package (ver. 1.0.8). For Gene Set
604 Enrichment Analysis (GSEA), all transcripts within annotated genes (~14,404 features in
605 total) regarding expression values were uploaded to locally-installed GSEA software (ver.
606 4.2.3)⁷⁰. These transcripts were used for enrichment analysis in the C2 curated gene sets
607 (Canonical pathways) and GO Biological Process ontology from the Molecular Signature
608 Database (MSigDB). The reported GSEA outputs were filtered based on $p < 0.05$ and
609 normalized enrichment score (NES) > 1.3 . Pathway analysis was conducted using Metascape
610 web-based platform⁶⁹. Significant pathways were identified using DEGs and selected with p
611 < 0.05 and enrichment score (ES) > 1.5 .

612 **Metabolic analysis**

613 To profile the metabolic state of the cells, CD14⁺ monocytes were seeded onto
614 XFe24 cell culture plates (Seahorse Bioscience, Lexington, MA) with RPMI medium with
615 10% HS, followed by the induction of trained immunity for 6 days as described in Fig. 1A.
616 Metabolic analysis on IS-trained macrophages was performed according to the
617 manufacturer's instructions. For the glycolysis stress test, culture media was replaced with
618 Seahorse XF Base media supplemented with 2 mM L-glutamine (pH7.4) and incubated for 1
619 hr in the non-CO2 incubator. Glucose (10 mM), oligomycin (2 μ M), and 2-DG (50 mM, all
620 from Sigma-Aldrich) were sequentially used to treat cells during real-time measurements of
621 extracellular acidification rate (ECAR) using Seahorse XFe24 Analyzer (Seahorse
622 Bioscience). For the mito stress test, cells were incubated with Seahorse XF Base media
623 supplemented with 1 mM pyruvate, 2 mM L-glutamine, and 10 mM glucose (pH7.4) for 1 hr
624 in the non-CO2 incubator. Oligomycin (1.5 μ M), FCCP (2 μ M), and rotenone/antimycin A
625 (0.5 μ M, all from Sigma-Aldrich) were sequentially used to treat cells during real-time
626 measurements of oxygen consumption rate (OCR) using the Seahorse XFe24 Analyzer.
627 Parameters of glycolysis stress test and mito stress test were calculated using Seahorse XF
628 glycolysis or the mito stress test report generator program that was provided by the
629 manufacturer.

630 **Immunoblot analysis**

631 Total proteins were prepared using radioimmunoprecipitation assay (RIPA) buffer
632 (150 mM NaCl, 10 mM Na₂HPO₄, 0.5% sodium deoxycholate, 1% NP-40) containing a
633 protease and phosphatase inhibitor cocktail (Thermo Fisher Scientific, Waltham, MA, USA).

634 Cell lysates were separated on an 8-12% SDS-polyacrylamide gel and blotted onto a
635 polyvinylidene difluoride (PVDF) membrane (Bio-Rad, Hercules, CA, USA), The membrane
636 was incubated overnight at 4°C with primary Abs, such as anti-AhR, anti-ALOX5, and anti-
637 ALOX5AP/FLAP, followed by incubation with peroxidase-conjugated secondary Abs for 1 h.
638 The membranes were developed using the enhanced chemiluminescence (ECL) system.

639 **WST (Water Soluble Tetrazolium Salt) assay**

640 To test cell viability, IS-trained macrophages were re-stimulated with LPS for 24 hr.
641 Culture media was changed with serum-free RPMI medium and the WST reagent (EZ-
642 CYTOX, DoGenBio, Seoul, Korea) followed by incubation for 1-2 h. Measurement of the
643 optical density value (450 nm) was performed by Infinite M200 (Tecan).

644 **Mouse *in vivo* studies**

645 For *in vivo* experiments, C57BL/6 mice (7-8 weeks) were injected intraperitoneally
646 with 200 mg/kg IS in 100 µl PBS daily for 5 days. Another five days after IS injection, 5
647 mg/kg LPS (Sigma-Aldrich) were injected intraperitoneally 75 min prior to sacrifice. Whole
648 blood was incubated at RT for 30 min and centrifuged at 3,000 g for 10 min at 4°C to collect
649 mouse serum. The amount of TNF- α and IL-6 in serum was quantified using commercial
650 mouse ELISA kits (Thermo Fisher Scientific). For *ex vivo* experiments using splenic myeloid
651 cells, IS-trained mice were sacrificed and their spleens were aseptically collected. Single-cell
652 splenic suspensions were prepared in PBS after passage through a 40 µm cell strainer.
653 Splenocytes were seeded at 1×10^7 cells/well in 12-well plates. After incubation for 1 h,
654 adherent cells were harvested for immunoblot analysis or stimulated with 10 ng/ml LPS for
655 24 hr. The amount of TNF- α and IL-6 in culture supernatants was quantified using

656 commercial mouse ELISA kits (Thermo Fisher Scientific).

657 **Statistics**

658 A two-tailed paired or unpaired non-parametric *t*-test was performed to analyze data using
659 Prism 8 (GraphPad Software, La Jolla, CA, USA) and Microsoft Excel 2013. *P* values of less
660 than 0.05 were considered statistically significant.

661 **AUTHOR CONTRIBUTIONS**

662 H. Y. Kim: conceived of the study, participated in its design and coordination, performed most
663 of the experiments, data collection, and analysis, wrote manuscript and provided financial
664 support. D. H. Kim, S. J. Lee, Y. J. Kang, and G. Kim: performed the experiments and data
665 analysis. H. M. Shin: participated in its design and performed data analysis. H. Lee and T.-H.
666 Yoo: conceived of the study, participated in its design, collected patient samples and clinical
667 information, and performed data analysis. W-W.L.: conceived of the study, participated in its
668 design and coordination, performed data analysis and writing of manuscript, and has full access
669 to all the data in this study and financial support. All authors have read and approved the final
670 manuscript.

671 **ACKNOWLEDGMENTS**

672 The authors thank Jiyeon Jang (Seoul National University College of Medicine) for assisting
673 in the recruitment of human subjects and thank the Core Lab, Clinical Trials Center, Seoul
674 National University Hospital for drawing blood. This work was supported in part by a grant
675 (Grant no: 2022R1A4A1033767 and 2022R1A2C3011243 to W-W. Lee) from the National
676 Research Foundation of Korea (NRF) funded by Ministry of Science and ICT (MSIT) and by
677 a grant (Grant no: NRF-2020R1I1A1A01063010 to H.Y.K.) of Basic Science Research
678 Program through NRF funded by the Ministry of Education, Republic of Korea.

679 **CONFLICT OF INTEREST**

680 The authors declare that they have no conflicts of interest with the contents of this article.

681 **REFERENCES**

- 682 1. Netea MG, Quintin J, van der Meer JW. Trained immunity: a memory for innate host
683 defense. *Cell Host Microbe* **9**, 355-361 (2011).
684
- 685 2. Netea MG, *et al.* Trained immunity: A program of innate immune memory in health
686 and disease. *Science (New York, NY)* **352**, aaf1098 (2016).
687
- 688 3. Netea MG, *et al.* Defining trained immunity and its role in health and disease. *Nature*
689 *reviews Immunology* **20**, 375-388 (2020).
690
- 691 4. Arts RJ, *et al.* Glutaminolysis and Fumarate Accumulation Integrate Immunometabolic
692 and Epigenetic Programs in Trained Immunity. *Cell metabolism* **24**, 807-819 (2016).
693
- 694 5. Bekkering S, *et al.* Metabolic Induction of Trained Immunity through the Mevalonate
695 Pathway. *Cell* **172**, 135-146.e139 (2018).
696
- 697 6. Cheng SC, *et al.* mTOR- and HIF-1 α -mediated aerobic glycolysis as metabolic basis
698 for trained immunity. *Science (New York, NY)* **345**, 1250684 (2014).
699
- 700 7. Saeed S, *et al.* Epigenetic programming of monocyte-to-macrophage differentiation and
701 trained innate immunity. *Science (New York, NY)* **345**, 1251086 (2014).
702
- 703 8. Christ A, *et al.* Western Diet Triggers NLRP3-Dependent Innate Immune
704 Reprogramming. *Cell* **172**, 162-175.e114 (2018).
705
- 706 9. Fanucchi S, *et al.* Immune genes are primed for robust transcription by proximal long
707 noncoding RNAs located in nuclear compartments. *Nat Genet* **51**, 138-150 (2019).
708
- 709 10. Edgar L, *et al.* Hyperglycemia Induces Trained Immunity in Macrophages and Their
710 Precursors and Promotes Atherosclerosis. *Circulation* **144**, 961-982 (2021).
711
- 712 11. Jenthoe E, *et al.* Trained innate immunity, long-lasting epigenetic modulation, and
713 skewed myelopoiesis by heme. *Proc Natl Acad Sci U S A* **118**, (2021).
714
- 715 12. Bekkering S, Quintin J, Joosten LA, van der Meer JW, Netea MG, Riksen NP. Oxidized
716 low-density lipoprotein induces long-term proinflammatory cytokine production and
717 foam cell formation via epigenetic reprogramming of monocytes. *Arterioscler Thromb*
718 *Vasc Biol* **34**, 1731-1738 (2014).
719
- 720 13. van der Valk FM, *et al.* Oxidized Phospholipids on Lipoprotein(a) Elicit Arterial Wall
721 Inflammation and an Inflammatory Monocyte Response in Humans. *Circulation* **134**,
722 611-624 (2016).
723
- 724 14. Arts RJW, *et al.* BCG Vaccination Protects against Experimental Viral Infection in
725 Humans through the Induction of Cytokines Associated with Trained Immunity. *Cell*
726 *Host Microbe* **23**, 89-100 e105 (2018).
727

- 728 15. Mulder WJM, Ochando J, Joosten LAB, Fayad ZA, Netea MG. Therapeutic targeting
729 of trained immunity. *Nat Rev Drug Discov* **18**, 553-566 (2019).
730
- 731 16. Cabău G, Crișan TO, Klück V, Popp RA, Joosten LAB. Urate-induced immune
732 programming: Consequences for gouty arthritis and hyperuricemia. *Immunological*
733 *reviews* **294**, 92-105 (2020).
734
- 735 17. Chen TK, Knicely DH, Grams ME. Chronic Kidney Disease Diagnosis and
736 Management: A Review. *Jama* **322**, 1294-1304 (2019).
737
- 738 18. Couser WG, Remuzzi G, Mendis S, Tonelli M. The contribution of chronic kidney
739 disease to the global burden of major noncommunicable diseases. *Kidney Int* **80**, 1258-
740 1270 (2011).
741
- 742 19. Vanholder R, *et al.* Review on uremic toxins: classification, concentration, and
743 interindividual variability. *Kidney Int* **63**, 1934-1943 (2003).
744
- 745 20. Kato S, *et al.* Aspects of immune dysfunction in end-stage renal disease. *Clin J Am Soc*
746 *Nephrol* **3**, 1526-1533 (2008).
747
- 748 21. Kim HY, *et al.* Indoxyl sulfate (IS)-mediated immune dysfunction provokes endothelial
749 damage in patients with end-stage renal disease (ESRD). *Scientific reports* **7**, 3057
750 (2017).
751
- 752 22. Duranton F, *et al.* Normal and pathologic concentrations of uremic toxins. *Journal of*
753 *the American Society of Nephrology : JASN* **23**, 1258-1270 (2012).
754
- 755 23. Lim YJ, Sidor NA, Tonial NC, Che A, Urquhart BL. Uremic Toxins in the Progression
756 of Chronic Kidney Disease and Cardiovascular Disease: Mechanisms and Therapeutic
757 Targets. *Toxins* **13**, (2021).
758
- 759 24. Gao H, Liu S. Role of uremic toxin indoxyl sulfate in the progression of cardiovascular
760 disease. *Life Sci* **185**, 23-29 (2017).
761
- 762 25. Kim HY, Yoo TH, Cho JY, Kim HC, Lee WW. Indoxyl sulfate-induced TNF- α is
763 regulated by crosstalk between the aryl hydrocarbon receptor, NF- κ B, and SOCS2 in
764 human macrophages. *FASEB journal : official publication of the Federation of*
765 *American Societies for Experimental Biology* **33**, 10844-10858 (2019).
766
- 767 26. Nakano T, *et al.* Uremic Toxin Indoxyl Sulfate Promotes Proinflammatory Macrophage
768 Activation Via the Interplay of OATP2B1 and Dll4-Notch Signaling. *Circulation* **139**,
769 78-96 (2019).
770
- 771 27. Bekkering S, Blok BA, Joosten LA, Riksen NP, van Crevel R, Netea MG. In Vitro
772 Experimental Model of Trained Innate Immunity in Human Primary Monocytes. *Clin*
773 *Vaccine Immunol* **23**, 926-933 (2016).
774

- 775 28. Divangahi M, *et al.* Trained immunity, tolerance, priming and differentiation: distinct
776 immunological processes. *Nature immunology* **22**, 2-6 (2021).
777
- 778 29. Gourbal B, Pinaud S, Beckers GJM, Van Der Meer JWM, Conrath U, Netea MG. Innate
779 immune memory: An evolutionary perspective. *Immunological reviews* **283**, 21-40
780 (2018).
781
- 782 30. Stevens PE, Levin A. Evaluation and management of chronic kidney disease: synopsis
783 of the kidney disease: improving global outcomes 2012 clinical practice guideline.
784 *Annals of internal medicine* **158**, 825-830 (2013).
785
- 786 31. Harbower DM, *et al.* Ornithine decarboxylase regulates M1 macrophage activation
787 and mucosal inflammation via histone modifications. *Proceedings of the National*
788 *Academy of Sciences* **114**, E751-E760 (2017).
789
- 790 32. Fanucchi S, Dominguez-Andres J, Joosten LAB, Netea MG, Mhlanga MM. The
791 Intersection of Epigenetics and Metabolism in Trained Immunity. *Immunity* **54**, 32-43
792 (2021).
793
- 794 33. Schroeder JC, *et al.* The uremic toxin 3-indoxyl sulfate is a potent endogenous agonist
795 for the human aryl hydrocarbon receptor. *Biochemistry* **49**, 393-400 (2010).
796
- 797 34. Brito JS, Borges NA, Esgalhado M, Magliano DC, Soulage CO, Mafra D. Aryl
798 Hydrocarbon Receptor Activation in Chronic Kidney Disease: Role of Uremic Toxins.
799 *Nephron* **137**, 1-7 (2017).
800
- 801 35. Dou L, *et al.* Aryl hydrocarbon receptor is activated in patients and mice with chronic
802 kidney disease. *Kidney Int* **93**, 986-999 (2018).
803
- 804 36. Salina ACG, *et al.* Leukotriene B(4) licenses inflammasome activation to enhance skin
805 host defense. *Proc Natl Acad Sci U S A* **117**, 30619-30627 (2020).
806
- 807 37. Rådmark O, Werz O, Steinhilber D, Samuelsson B. 5-Lipoxygenase: regulation of
808 expression and enzyme activity. *Trends in biochemical sciences* **32**, 332-341 (2007).
809
- 810 38. Pernet E, Downey J, Vinh DC, Powell WS, Divangahi M. Leukotriene B(4)-type I
811 interferon axis regulates macrophage-mediated disease tolerance to influenza infection.
812 *Nature microbiology* **4**, 1389-1400 (2019).
813
- 814 39. Kim HY, *et al.* Indoxyl Sulfate-Mediated Metabolic Alteration of Transcriptome
815 Signatures in Monocytes of Patients with End-Stage Renal Disease (ESRD). *Toxins* **12**,
816 (2020).
817
- 818 40. Kimball AS, *et al.* The Histone Methyltransferase Setdb2 Modulates Macrophage
819 Phenotype and Uric Acid Production in Diabetic Wound Repair. *Immunity* **51**, 258-
820 271.e255 (2019).
821

- 822 41. Zhong Q, Gong FY, Gong Z, Hua SH, Zeng KQ, Gao XM. IgG Immunocomplexes
823 Sensitize Human Monocytes for Inflammatory Hyperactivity via Transcriptomic and
824 Epigenetic Reprogramming in Rheumatoid Arthritis. *J Immunol* **200**, 3913-3925 (2018).
825
- 826 42. Keating ST, *et al.* The Set7 Lysine Methyltransferase Regulates Plasticity in Oxidative
827 Phosphorylation Necessary for Trained Immunity Induced by beta-Glucan. *Cell Rep* **31**,
828 107548 (2020).
829
- 830 43. Bekkering S, Dominguez-Andres J, Joosten LAB, Riksen NP, Netea MG. Trained
831 Immunity: Reprogramming Innate Immunity in Health and Disease. *Annu Rev Immunol*
832 **39**, 667-693 (2021).
833
- 834 44. Netea MG, Schlitzer A, Placek K, Joosten LAB, Schultze JL. Innate and Adaptive
835 Immune Memory: an Evolutionary Continuum in the Host's Response to Pathogens.
836 *Cell Host Microbe* **25**, 13-26 (2019).
837
- 838 45. Giamarellos-Bourboulis EJ, *et al.* Activate: Randomized Clinical Trial of BCG
839 Vaccination against Infection in the Elderly. *Cell* **183**, 315-323.e319 (2020).
840
- 841 46. O'Neill LAJ, Netea MG. BCG-induced trained immunity: can it offer protection against
842 COVID-19? *Nature reviews Immunology* **20**, 335-337 (2020).
843
- 844 47. Buffen K, *et al.* Autophagy controls BCG-induced trained immunity and the response
845 to intravesical BCG therapy for bladder cancer. *PLoS Pathog* **10**, e1004485 (2014).
846
- 847 48. Menon V, Gul A, Sarnak MJ. Cardiovascular risk factors in chronic kidney disease.
848 *Kidney Int* **68**, 1413-1418 (2005).
849
- 850 49. Hung SC, Kuo KL, Wu CC, Tarng DC. Indoxyl Sulfate: A Novel Cardiovascular Risk
851 Factor in Chronic Kidney Disease. *Journal of the American Heart Association* **6**,
852 (2017).
853
- 854 50. Sarnak MJ, *et al.* Kidney disease as a risk factor for development of cardiovascular
855 disease: a statement from the American Heart Association Councils on Kidney in
856 Cardiovascular Disease, High Blood Pressure Research, Clinical Cardiology, and
857 Epidemiology and Prevention. *Circulation* **108**, 2154-2169 (2003).
858
- 859 51. Betjes MG. Immune cell dysfunction and inflammation in end-stage renal disease. *Nat*
860 *Rev Nephrol* **9**, 255-265 (2013).
861
- 862 52. Leong SC, Sirich TL. Indoxyl Sulfate—Review of Toxicity and Therapeutic Strategies.
863 *Toxins* **8**, 358 (2016).
864
- 865 53. Barisione C, *et al.* Moderate Increase of Indoxyl Sulfate Promotes Monocyte Transition
866 into Profibrotic Macrophages. *PLoS One* **11**, e0149276 (2016).
867
- 868 54. Rothhammer V, Quintana FJ. The aryl hydrocarbon receptor: an environmental sensor

- 869 integrating immune responses in health and disease. *Nature reviews Immunology* **19**,
870 184-197 (2019).
871
- 872 55. Stockinger B, Di Meglio P, Gialitakis M, Duarte JH. The aryl hydrocarbon receptor:
873 multitasking in the immune system. *Annu Rev Immunol* **32**, 403-432 (2014).
874
- 875 56. Bock KW. Aryl hydrocarbon receptor (AHR) functions in infectious and sterile
876 inflammation and NAD(+)-dependent metabolic adaptation. *Arch Toxicol* **95**, 3449-
877 3458 (2021).
878
- 879 57. Duarte-Hospital C, *et al.* Mitochondrial Dysfunction as a Hallmark of Environmental
880 Injury. *Cells* **11**, (2021).
881
- 882 58. Gutierrez-Vazquez C, Quintana FJ. Regulation of the Immune Response by the Aryl
883 Hydrocarbon Receptor. *Immunity* **48**, 19-33 (2018).
884
- 885 59. Nakano T, *et al.* Indoxyl Sulfate Contributes to mTORC1-Induced Renal Fibrosis via
886 The OAT/NADPH Oxidase/ROS Pathway. *Toxins* **13**, (2021).
887
- 888 60. Ihara A, Wada K, Yoneda M, Fujisawa N, Takahashi H, Nakajima A. Blockade of
889 leukotriene B4 signaling pathway induces apoptosis and suppresses cell proliferation
890 in colon cancer. *J Pharmacol Sci* **103**, 24-32 (2007).
891
- 892 61. Tong WG, Ding XZ, Talamonti MS, Bell RH, Adrian TE. LTB4 stimulates growth of
893 human pancreatic cancer cells via MAPK and PI-3 kinase pathways. *Biochem Biophys*
894 *Res Commun* **335**, 949-956 (2005).
895
- 896 62. Takeda T, *et al.* Dioxin-induced increase in leukotriene B4 biosynthesis through the
897 aryl hydrocarbon receptor and its relevance to hepatotoxicity owing to neutrophil
898 infiltration. *Journal of Biological Chemistry* **292**, 10586-10599 (2017).
899
- 900 63. Maccarrone M, *et al.* Arachidonate cascade, apoptosis, and vitamin E in peripheral
901 blood mononuclear cells from hemodialysis patients. *Am J Kidney Dis* **40**, 600-610
902 (2002).
903
- 904 64. Maccarrone M, *et al.* Vitamin E suppresses 5-lipoxygenase-mediated oxidative stress
905 in peripheral blood mononuclear cells of hemodialysis patients regardless of
906 administration route. *Am J Kidney Dis* **37**, 964-969 (2001).
907
- 908 65. Montford JR, *et al.* Inhibition of 5-lipoxygenase decreases renal fibrosis and
909 progression of chronic kidney disease. *Am J Physiol Renal Physiol* **316**, F732-f742
910 (2019).
911
- 912 66. Garcia-Valtanen P, Guzman-Genuino RM, Williams DL, Hayball JD, Diener KR.
913 Evaluation of trained immunity by beta-1, 3 (d)-glucan on murine monocytes in vitro
914 and duration of response in vivo. *Immunol Cell Biol* **95**, 601-610 (2017).
915

- 916 67. Rapa SF, *et al.* Pro-Inflammatory Effects of Indoxyl Sulfate in Mice: Impairment of
917 Intestinal Homeostasis and Immune Response. *Int J Mol Sci* **22**, (2021).
918
- 919 68. Arts RJW, *et al.* Immunometabolic Pathways in BCG-Induced Trained Immunity. *Cell*
920 *Rep* **17**, 2562-2571 (2016).
921
- 922 69. Zhou Y, *et al.* Metascape provides a biologist-oriented resource for the analysis of
923 systems-level datasets. *Nat Commun* **10**, 1523 (2019).
924
- 925 70. Subramanian A, *et al.* Gene set enrichment analysis: a knowledge-based approach for
926 interpreting genome-wide expression profiles. *Proc Natl Acad Sci U S A* **102**, 15545-
927 15550 (2005).
928

929 **FIGURE LEGENDS**

930 **Figure 1. IS induces trained immunity in human monocytes. A.** Schematic of *in vitro*
931 experimental model for innate trained immunity. **B-C.** Human monocytes were treated with
932 the indicated concentration of IS for 24 hr, followed by a subsequent 5-day culture in human
933 serum. On day 6, the cells were restimulated with the indicated concentrations of LPS for 24
934 hr. TNF- α and IL-6 proteins levels were quantified by ELISA. **D.** After training with 1,000
935 μ M IS, monocytes were restimulated with 10 μ g/ml Pam3cys. TNF- α and IL-6 protein levels
936 were quantified by ELISA. **E.** After training with 1,000 μ M IS, monocytes were restimulated
937 with 10 ng/ml LPS for 24 hr. The mRNA expression of IL-1 β , IL-10, and MCP-1 was
938 analyzed by RT-qPCR. Bar graphs show the mean \pm SEM. * = $p < 0.05$, and ** = $p < 0.01$ by
939 two-tailed paired *t*-test.

940 **Figure 2. IS-induced trained immunity is accomplished through epigenetic modification.**
941 **A.** Experimental scheme of ChIP-qPCR for IS-trained macrophages. **B.** On day 6 after IS-
942 training, cells were fixed with 1% formaldehyde, lysed, and sonicated. A ChIP assay was
943 performed using anti-H3K4me3 antibody and enrichment of H3K4me3 in the promoter site
944 of *TNFA* and *IL6* loci was quantified by qPCR. 1% input was used as a normalization control.
945 **C.** Monocytes were pre-treated with 5'-methylthioadenosine (MTA, a non-selective
946 methyltransferase inhibitor) and then were trained with IS for 6 days, followed by
947 restimulation with LPS for 24 hrs. TNF- α and IL-6 proteins levels were quantified by ELISA.
948 **D.** ChIP-Seq analysis was performed with anti-H3K4me3 antibody on chromatin isolated at
949 day 6 from IS-trained and control macrophages. Enriched peaks in ChIP-Seq on H3K4me3
950 are shown as a volcano plot. (FC > 1.3, $p < 0.05$) **E.** Functional annotation of 59 upregulated
951 Differentially regulated peaks (DRPs) on H3K4me3 in IS-trained macrophages were

952 analyzed by Gene Ontology (Go) analysis with Go biological pathway and Reactome gene
953 sets ($FC > 1.3$, $p < 0.05$). **F.** Screen shots of H3K4me3 modification in the promoter regions
954 of IFI16, XRCC5, PQBP1 PSMA1, PSMA3, and OAZ3. $* = p < 0.05$, $** = p < 0.01$, and $*** =$
955 $p < 0.001$ by two-tailed paired t -test.

956 **Figure 3. IS-induced trained immunity is linked to metabolic rewiring.** Glycolysis and
957 mitochondrial stress tests were conducted on IS-trained macrophages ($n = 3\sim 4$) using the
958 Seahorse XF-analyzer. **A.** ECAR (extracellular acidification rate) levels were measured after
959 sequential treatment with glucose, oligomycin, and 2-DG. **B.** Cellular glycolysis and
960 glycolytic capacity were analyzed. **C.** OCR (Oxygen consumption rate) levels were measured
961 after sequential treatment with oligomycin, FCCP, and Rotenone/antimycin A (Ro/AA). **D.**
962 Basal respiration, maximal respiration, and ATP production were analyzed. **E.** Monocytes
963 were pretreated with 2DG, followed by IS-training for 6 days. Cells were restimulated with
964 LPS for 24 hr and TNF- α and IL-6 in supernatants were quantified by ELISA ($n = 5$). Bar
965 graphs show the mean \pm SEM. $* = p < 0.05$, $** = p < 0.01$, and $*** = p < 0.001$ by two-tailed
966 paired t -test.

967 **Figure 4. IS-induced trained immunity is regulated by AhR.** Monocytes were pretreated
968 with or without GNF351 (AhR antagonist) followed by IS-training for 6 days. **A.** On day 6,
969 cell lysates were prepared and immunoblotted for AhR protein. Band intensity in
970 immunoblots was quantified by densitometry. β -actin was used as a normalization control. **B-**
971 **D.** On day 6, IS-trained cells with or without GNF351 were restimulated with LPS for 24 hr.
972 TNF- α and IL-6 in supernatants were quantified by ELISA (B). Expression of TNF- α and IL-
973 6 (C) and IL-1 β , MCP-1, and IL-10 mRNA (D) was analyzed by RT-qPCR. **E.** Enrichment of
974 H3K4me3 on promoters of *TNFA* and *IL6* loci was assessed on day 6 after IS-training. 1%

975 input was used as a normalization control. Bar graphs show the mean \pm SEM. * = $p < 0.05$,
976 ** = $p < 0.01$, and *** = $p < 0.001$ by two-tailed paired *t*-test.

977 **Figure 5. AhR-dependent induction of the arachidonic acid pathway contributes to IS-**
978 **induced trained immunity. A-B.** RNA-Seq analysis was performed on IS-trained
979 monocytes. Heatmaps (A) and volcano plots (B) show differentially expressed genes between
980 IS-trained and non-trained macrophages. **C.** Functional annotation of upregulated or
981 downregulated genes ($FC > \pm 2$, $p < 0.05$) in IS-trained macrophages analyzed by Gene
982 Ontology (GO) analysis with the Reactome Gene Set. **D-E.** GSEA (D) and heatmap (E) of
983 genes related to the AA metabolism in IS-trained macrophages compared to non-trained cells
984 or compared to IS-trained macrophages with GNF351 treatment were analyzed. **F-G.** On day
985 6 after IS-training with or without GNF351, expression of CYP1B1, ALOX5, ALOX5AP,
986 and LTB4R1 mRNAs were quantitated using RT-qPCR (F) and cell lysates were prepared and
987 immunoblotted for ALOX5 and ALOX5AP proteins (G). Band intensity in immunoblots was
988 quantified by densitometry. β -actin was used as a normalization control. **H-I.** Monocytes
989 were pretreated with zileuton (ALOX5 inhibitor) or U75302 (BLT1 inhibitor) and trained
990 with IS for 6 days followed by restimulation with LPS for 24 hr. TNF- α and IL-6 in
991 supernatants were quantified by ELISA. **J.** On day 6 after IS-training with or without MTA,
992 expression of ALOX5, ALOX5AP, and LTB4R1 mRNAs were quantified using RT-qPCR.
993 Bar graphs show the mean \pm SEM. * = $p < 0.05$, ** = $p < 0.01$, *** = $p < 0.001$ by two-tailed
994 paired *t*-test.

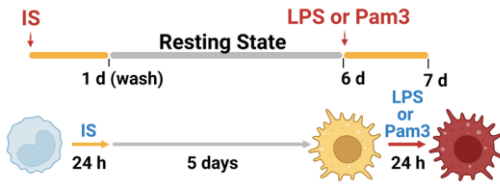
995 **Figure 6. Ex vivo and in vivo validation of IS-induced trained immunity. A-B.** The pooled
996 normal serum (NS) from healthy controls (HCs) or uremic serum (US) from patients with
997 ESRD were used for treatment of monocytes isolated from HCs for 24 hr at 30% (v/v) followed

998 by resting for 5 days. After stimulation with LPS for 24 hr, TNF- α and IL-6 production were
999 analyzed using ELISA (A) and RT-qPCR (B). **C.** Expression of ALOX5, ALOX5AP, and
1000 LTB4R1 mRNAs were quantitated using RT-qPCR in trained macrophages with NS or US for
1001 6 days. **D-G.** ALOX5 and ALOX5AP protein levels in monocytes (D-E) and HMDM (F-G) of
1002 ESRD patients and HC were analyzed by immunoblot analysis. Band intensity in immunoblots
1003 was quantified by densitometry. β -actin was used as a normalization control. **H.** C57BL/6 mice
1004 were injected daily with 200 mg/kg IS for 5 days and rested for another 5 days prior to LPS
1005 treatment. Mice were sacrificed at 75 min post-LPS injection. **I.** TNF- α and IL-6 in serum were
1006 quantified by ELISA. **J.** Before LPS injection, IS-trained mice were sacrificed and spleens
1007 were mechanically separated. Isolated splenic myeloid cells were treated *ex vivo* with 10 ng/ml
1008 LPS for 24 hr and TNF- α and IL-6 in supernatants were quantified by ELISA. **K.** The level of
1009 ALOX5 protein in splenic myeloid cells isolated from IS-trained or control mice was analyzed
1010 by western blot. The right panel shows the band intensity quantified by the densitometry. Bar
1011 graphs show the mean \pm SEM. * = $p < 0.05$, ** = $p < 0.01$, and *** = $p < 0.001$ by two-tailed
1012 paired *t*-test (A-C) or unpaired non-parametric *t*-test (E, G, I, J and K).

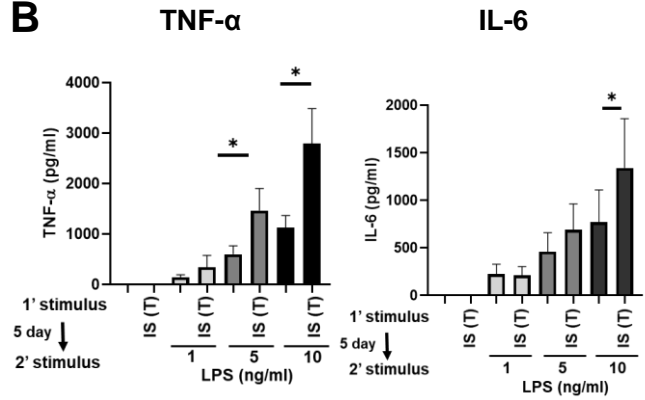
1013 **Figure 7. Proposed mechanism of IS-induced trained immunity.** Indoxyl sulfate, a uremic
1014 toxin, induces trained immunity of monocytes/macrophages through the AhR-dependent
1015 arachidonic acid pathway.

Figure 1

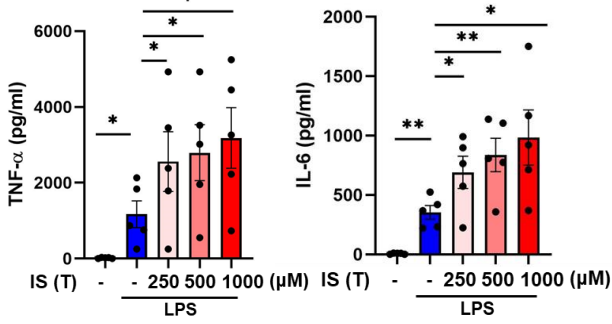
A



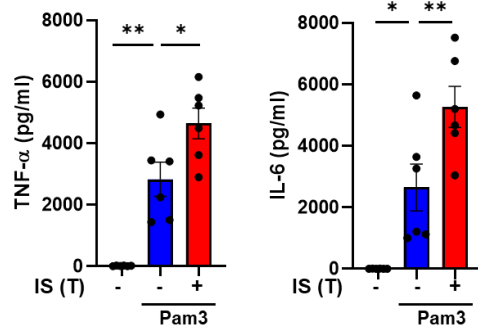
B



C



D



E

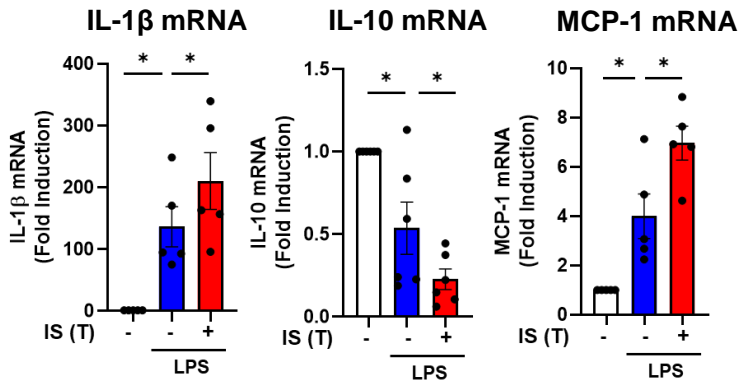
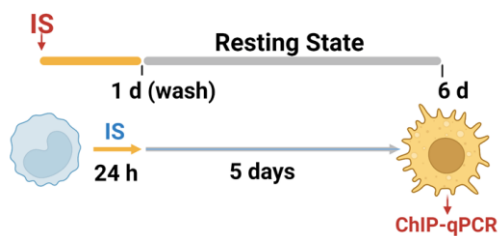
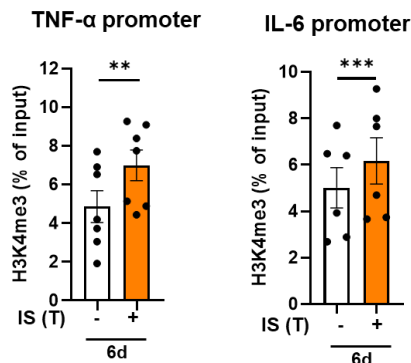


Figure 2

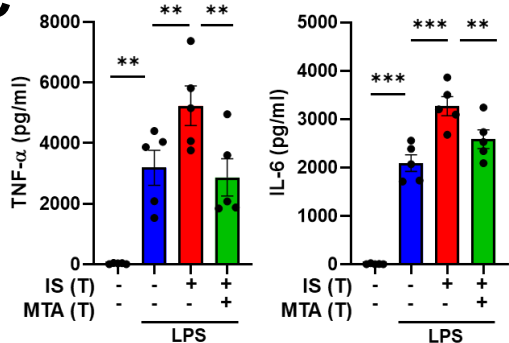
A



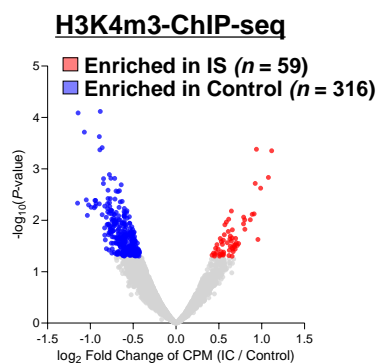
B



C

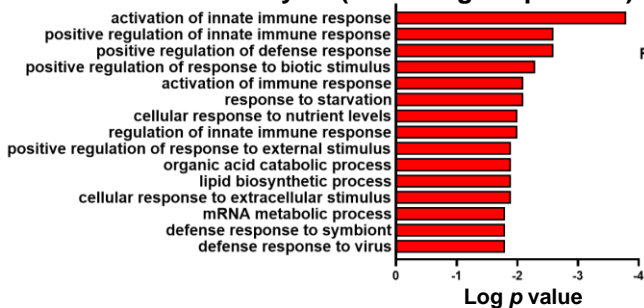


D

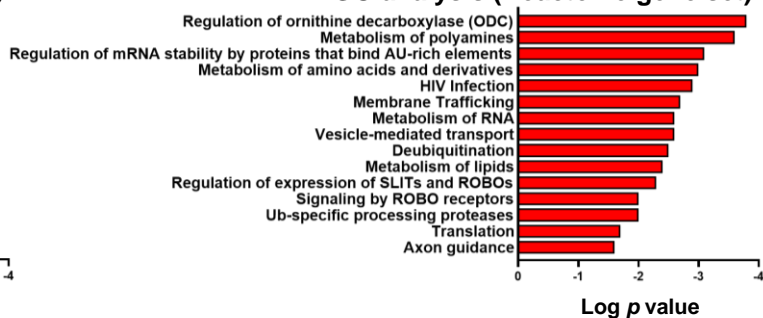


E

GO analysis (Go biological process)

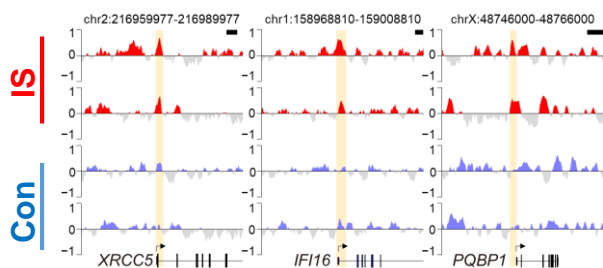


GO analysis (Reactome gene set)



F

activation of the innate immune response



Regulation of ornithine decarboxylase (ODC)

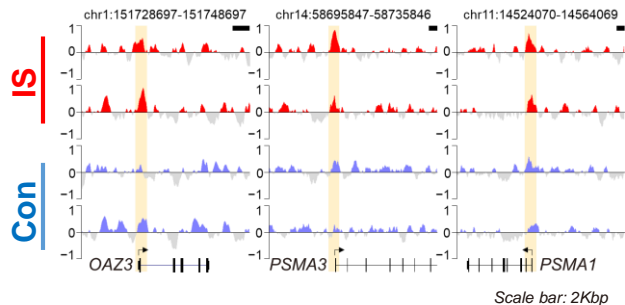


Figure 3

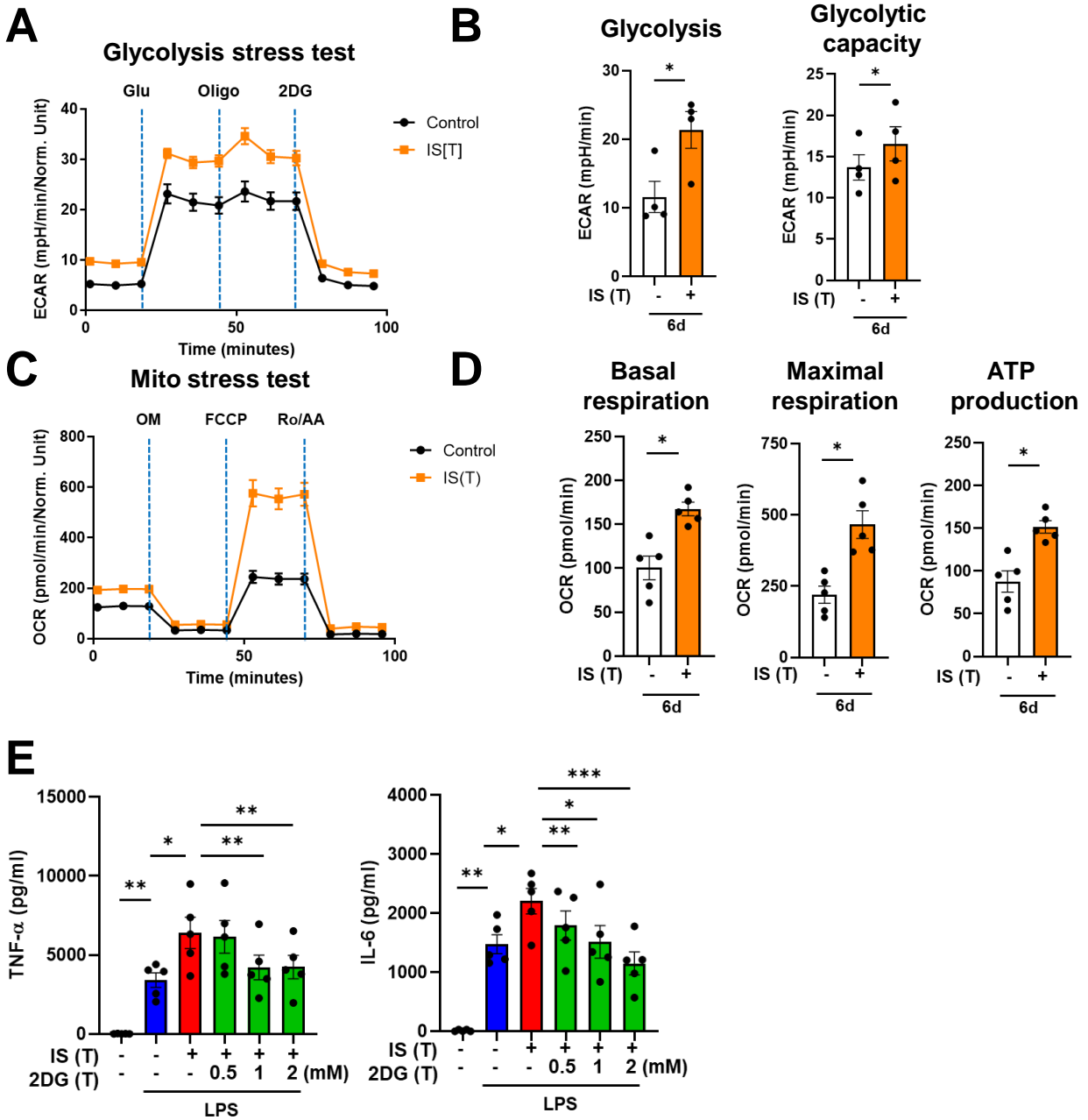
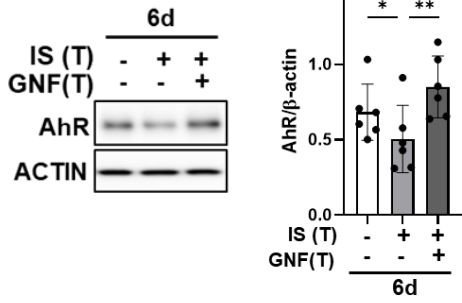
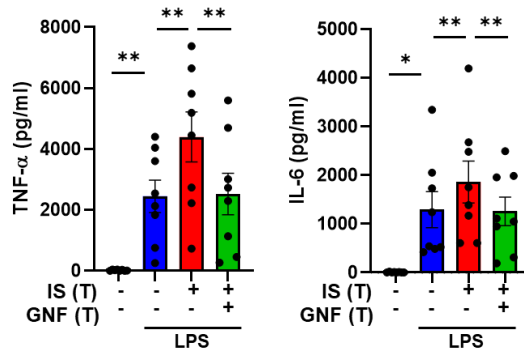


Figure 4

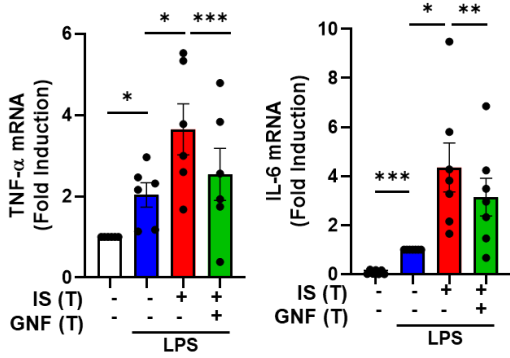
A



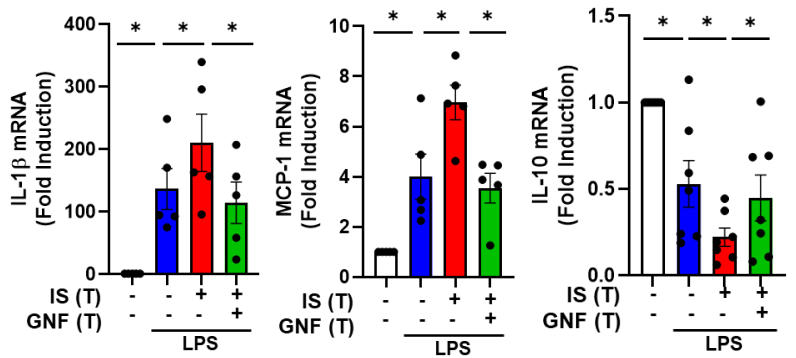
B



C



D



E

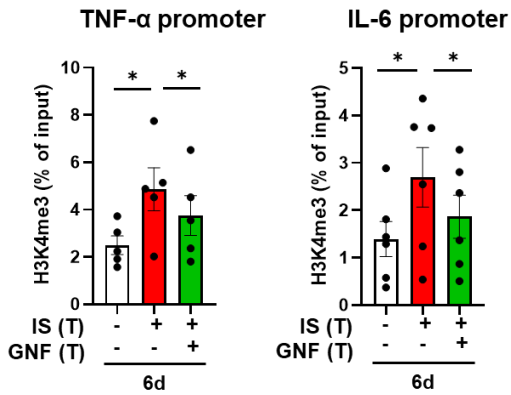
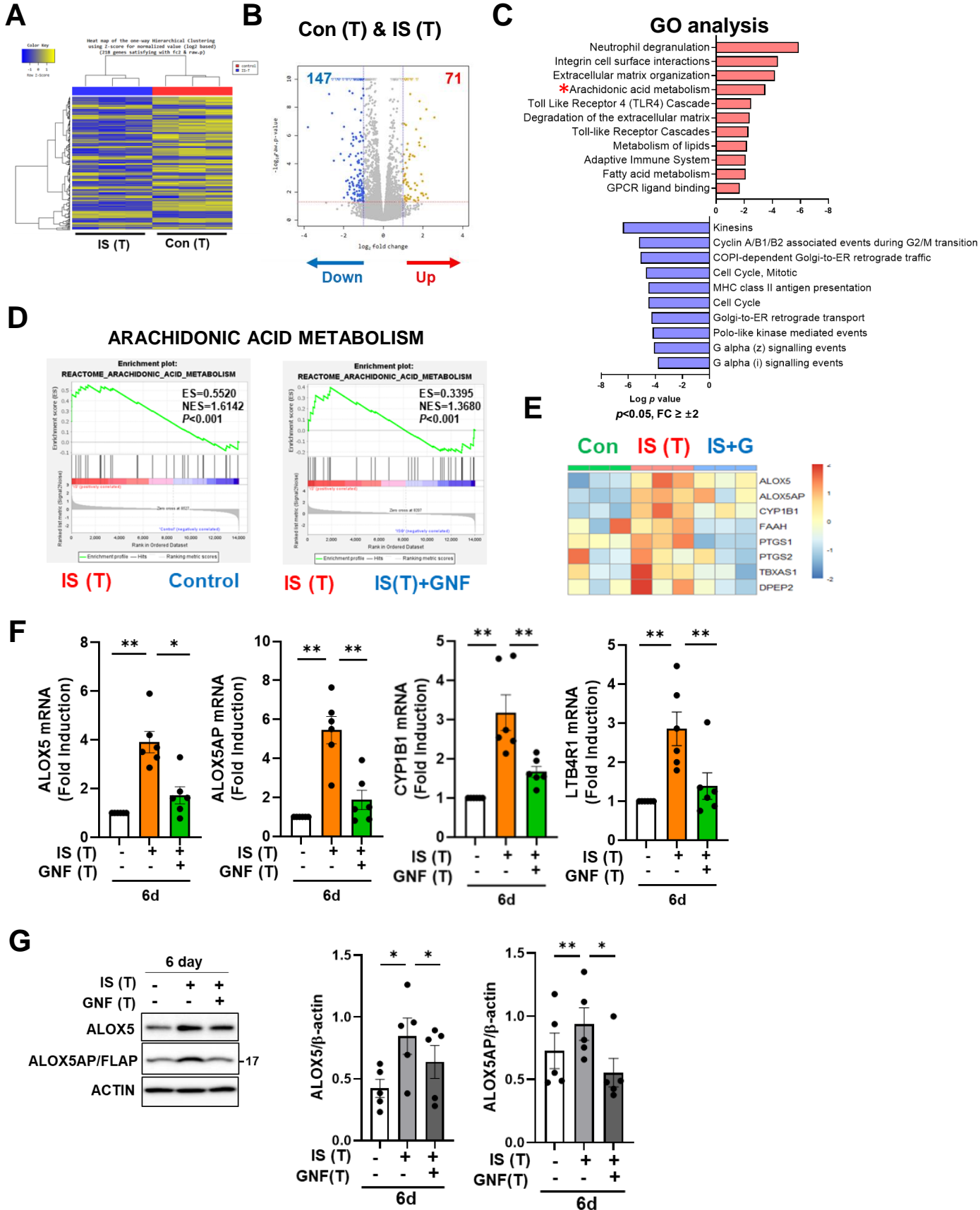


Figure 5



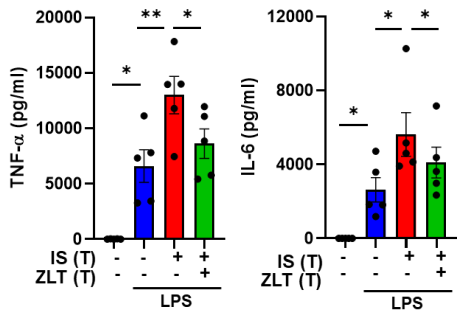
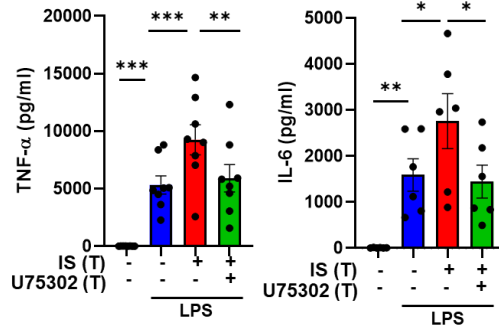
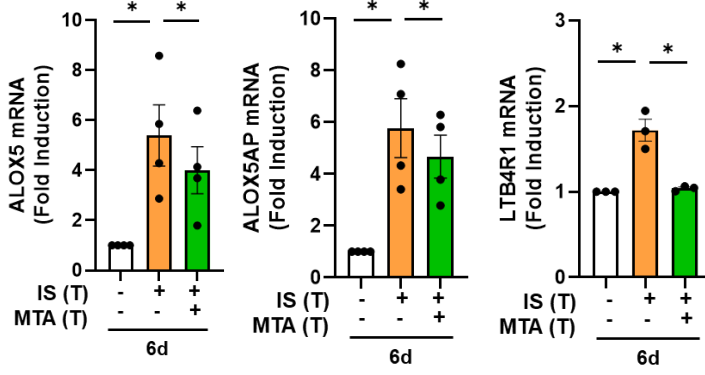
H**I****J**

Figure 6

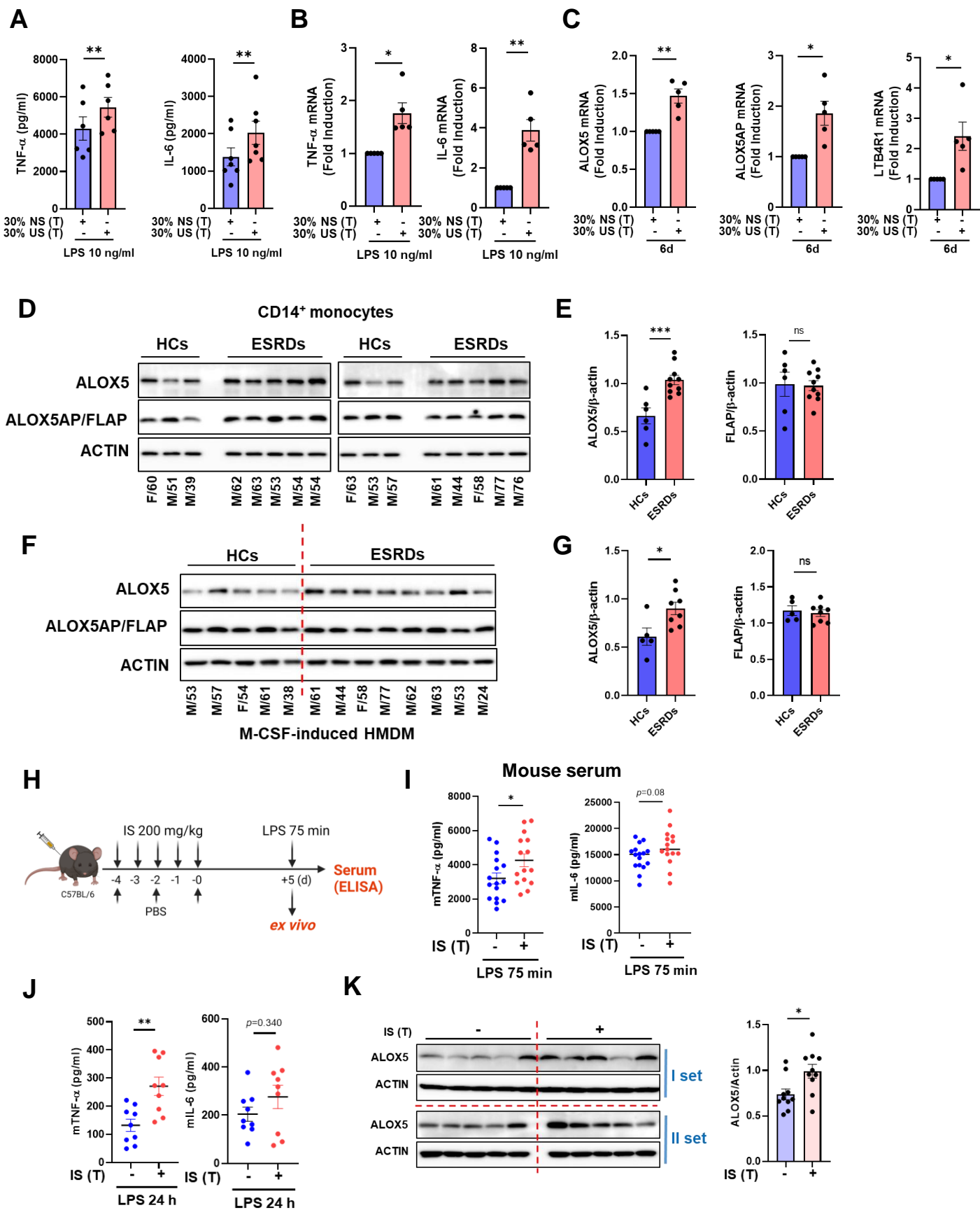


Figure 7

